

Higher order quasi-Monte Carlo for Bayesian shape inversion

R. N. Gantner, M. D. Peters

Departement Mathematik und Informatik
Fachbereich Mathematik
Universität Basel
CH-4051 Basel

Preprint No. 2016-18
September 2016

www.math.unibas.ch

Higher Order Quasi-Monte Carlo for Bayesian Shape Inversion*

R. N. Gantner[†] and M. D. Peters[‡]

Abstract. In this article, we consider a Bayesian approach towards data assimilation and uncertainty quantification in diffusion problems on random domains. We provide a rigorous analysis of parametric regularity of the posterior distribution given that the data exhibit only limited smoothness. Moreover, we present a dimension truncation analysis for the forward problem, which is formulated in terms of the domain mapping method. Having these novel results at hand, we shall consider as a practical example Electrical Impedance Tomography in the regime of constant conductivities. We are interested in computing moments, in particular expectation and variance, of the contour of an unknown inclusion, given perturbed surface measurements. By casting the forward problem into the framework of elliptic diffusion problems on random domains, we can directly apply the presented analysis. This straightforwardly yields parametric regularity results for the system response and for the posterior measure, facilitating the application of higher order quadrature methods for the approximation of moments of quantities of interest. As an example of such a quadrature method, we consider here recently developed higher order quasi-Monte Carlo methods. To solve the forward problem numerically, we employ a fast boundary integral solver. Numerical examples are provided to illustrate the presented approach and validate the theoretical findings.

Key words. Quasi-Monte Carlo methods, uncertainty quantification, error estimates, high dimensional quadrature, Electrical Impedance Tomography

AMS subject classifications. 65N21, 65N38, 65D30

1. Introduction. The present article considers the Bayesian approach, see e.g. [11, 13, 40], to assimilate measured data in the framework of elliptic diffusion equations on random domains. The forward problem is solved by means of the domain mapping method as it has been considered in [6, 27, 44]. In particular, we extend here the analysis presented in [27] and consider the impact of dimension truncation on the system response. In view of the computation of quantities of interest, the Bayesian approach boils down to the approximation of high-dimensional integrals. In order to apply the higher order quasi-Monte Carlo methods considered in [15, 21], we provide additionally a rigorous and general analysis of the posterior measure, for a uniform prior and additive Gaussian noise, in the regime where the system response provides only limited smoothness. This might occur in the present setting if the given data, like loadings and boundary data, exhibit only limited regularity. The presented analysis might be considered as an extension of previous works, see particularly [13, 27]. Having these prerequisites at hand, we shall consider Electrical Impedance Tomography (EIT) as a practical example. EIT is a non-invasive medical imaging procedure and has been extensively studied

*Submitted to the editors September 27, 2016.

Funding: This work was supported by the Swiss National Science Foundation (SNSF) under Grant No. SNF149819 to Christoph Schwab and by CPU time from the Swiss National Supercomputing Centre (CSCS) under project ID d41.

[†]ETH Zurich, Seminar for Applied Mathematics, Rämistrasse 101, CH-8092 Zurich, Switzerland (robert.gantner@sam.math.ethz.ch).

[‡]University of Basel, Department of Mathematics and Computer Science, Spiegelgasse 1, CH-4051 Basel, Switzerland (michael.peters@unibas.ch).

36 in the context of inverse problems, see e.g. [2, 3, 18, 19, 28]. Exploiting differences in the
 37 electrical conductivity among different biological tissues, EIT reconstructs and images these
 38 conductivities based on surface electrode measurements. In particular, we refer here to the case
 39 of constant conductivities, where the goal is to determine the shape of an unknown inclusion,
 40 see e.g. [5, 7, 24, 28, 33]. Especially in the absence of noise, it is possible to reconstruct the
 41 inclusion from a single pair of current/voltage measurements, cf. [5]. This is in contrast to
 42 the recent work [17], which also considers Bayesian inversion in the context of EIT. There,
 43 the authors reconstruct a diffusion coefficient (representing varying conductivities) from noisy
 44 measurements, instead of the shape of the domain.

45 Our goal will be to approximate the expected shape of an inclusion, given surface mea-
 46 surements from the domain's boundary. The Bayesian framework will allow also arbitrary
 47 moments to be computed, allowing specification of a “confidence interval” for the inclusion's
 48 shape. A major advantage of the model problem under consideration is that it can be effi-
 49 ciently solved by means of boundary integral equations as it has been done for example in
 50 [18]. This allows for numerical studies concerning the convergence behaviour of the applied
 51 higher order quasi-Monte Carlo quadrature.

52 The remainder of this article is structured as follows. In Section 2, we introduce the
 53 Bayesian formulation in a rather abstract fashion and parametric regularity results for the
 54 posterior measure are derived, given a general regularity estimate for the system response of
 55 the forward problem. After this, in Section 3, we present the forward model under consider-
 56 ation, i.e. diffusion problems on random domains, and provide an analysis for the impact of
 57 dimension truncation. Section 4 deals with the EIT problem and recasts it into the framework
 58 of a diffusion problem on a random domain. We comment also on the discretization by means
 59 of boundary integral equations. Interlaced polynomial lattice rules are briefly discussed in the
 60 subsequent Section 5, which are the higher-order quasi-Monte Carlo (HoQMC) methods we
 61 will use in the computations. In Section 6, a numerical experiment is formulated to compare
 62 HoQMC to conventional methods and the results are discussed.

63 2. Bayesian Inversion.

64 **2.1. The Bayesian Framework.** Let \mathcal{X} denote some real and separable Banach space
 65 and let $\mathcal{A}(\mathbf{y}): \mathcal{X} \rightarrow \mathcal{X}^*$ be a bounded linear operator for each given parameter sequence
 66 $\mathbf{y} \in U := [-1/2, 1/2]^{\mathbb{N}}$. For $f(\mathbf{y}) \in \mathcal{X}^*$, we consider the parameteric operator equation

$$67 \quad (1) \quad \mathcal{A}(\mathbf{y})q(\mathbf{y}) = f(\mathbf{y}).$$

68 We require that the system response q satisfies then a regularity estimate of the form

$$69 \quad (2) \quad \|\partial_{\mathbf{y}}^{\nu} q(\mathbf{y})\|_{\mathcal{X}} \leq C |\nu|! c^{|\nu|} \gamma^{\nu} \quad \text{for all } \nu \in \mathcal{F}_{\alpha},$$

70 where we denote by $C, c > 0$ constants which are independent of the sequence ν and $\gamma \in \ell^p(\mathbb{N})$
 71 for $p < 1$, and we use the convention $\gamma^{\nu} := \prod_{k \geq 1} \gamma_k^{\nu_k}$. The set \mathcal{F}_{α} is given by

$$72 \quad \mathcal{F}_{\alpha} := \left\{ \nu \in \mathbb{N}_0^{\mathbb{N}} : \nu \leq \alpha \right\}, \quad \text{where } \alpha \in \mathcal{F} := \left\{ \nu \in \mathbb{N}_0^{\mathbb{N}} : \sum_{k \geq 1} \nu_k < \infty \right\},$$

73 i.e. \mathcal{F}_α is the set of all finitely supported index sequences that are bounded by $\alpha \in \mathcal{F}$.
 74 Typically, such operator equations emerge from diffusion problems with random data, as
 75 random diffusion coefficients or right hand sides, see e.g. [4, 9], or even random domains [27].

76 Since there exists an $s \in \mathbb{N}$ such that $\nu_k = 0$ for all $k > s$ for all $\nu \in \mathcal{F}_\alpha$, we shall identify
 77 index sequences with multi indices $\nu = [\nu_1, \dots, \nu_s] \in \mathbb{N}^s$ without further notice.

78 Throughout what follows, we will assume the components of \mathbf{y} to be stochastically inde-
 79 pendent and identically uniformly distributed, i.e. we endow the set U with the structure of
 80 a probability space with respect to the product measure

$$81 \quad \mu_0(d\mathbf{y}) = \prod_{k \geq 1} dy_k.$$

82 This measure will be referred to as the *prior measure*. We denote by

$$83 \quad G: U \rightarrow \mathcal{X}, \quad \mathbf{y} \mapsto q(\mathbf{y})$$

84 the *uncertainty-to-solution map*, which maps a given instance $\mathbf{y} \in U$ of the parameter sequence
 85 to the corresponding solution $q(\mathbf{y}) \in \mathcal{X}$.

86 In forward UQ, the goal is to compute the expectation, with respect to the prior measure
 87 μ_0 , of a quantity of interest $\phi: \mathcal{X} \rightarrow \mathcal{Z}$, which is usually assumed to be a continuous linear
 88 functional of the parametric solution $q(\mathbf{y})$. The goal of Bayesian inverse UQ as in [11] is to
 89 incorporate noisy measurements of solutions to (12), after potentially incomplete observations.
 90 This is modeled by first considering a bounded, linear observation operator $\mathcal{O} \in \mathcal{L}(\mathcal{X}, Y)$ for
 91 a Banach space Y , which models e.g. point evaluation of the system response q , or averaging
 92 over a certain subdomain. In the following, we assume $Y = \mathbb{R}^K$ with $K < \infty$, i.e. we assume
 93 only finitely many measurements of the system response. Then, we define the *uncertainty-to-*
 94 *observation mapping* \mathcal{G} by

$$95 \quad (3) \quad \mathcal{G} = \mathcal{O} \circ G: U \rightarrow Y, \quad \mathbf{y} \mapsto \mathcal{G}(\mathbf{y}) = \mathcal{O}(q(\mathbf{y})).$$

96 The measured data δ is modeled as resulting from an observation by \mathcal{O} , perturbed with
 97 additive Gaussian noise, $\delta = \mathcal{O}(u(\mathbf{y}^*)) + \eta$, where \mathbf{y}^* is the unknown, exact parameter, and
 98 $\eta \sim \mathcal{N}(0, \Gamma)$. Hereby, we assume Γ to be a known symmetric, positive definite covariance
 99 matrix $\Gamma \in \mathbb{R}^{K \times K}$.

100 The goal will then be to predict expectations of the quantity of interest ϕ , which in general
 101 is an arbitrary continuous functional of the solution. In particular, it needs not contain the
 102 observation operator, thus allowing prediction of “unobservable” phenomena, given perturbed
 103 measurements of observable output. To that end, we define the Gaussian potential, also
 104 referred to as the least-squares or data misfit functional, by $\Phi_\Gamma: U \times Y \rightarrow \mathbb{R}$,

$$105 \quad (4) \quad \Phi_\Gamma(\mathbf{y}, \delta) := \frac{1}{2} \|\delta - \mathcal{G}(\mathbf{y})\|_\Gamma^2 = \frac{1}{2} (\delta - \mathcal{G}(\mathbf{y}))^\top \Gamma^{-1} (\delta - \mathcal{G}(\mathbf{y})).$$

106 Given the prior measure μ_0 , Bayes’ formula yields an expression for a *posterior measure*
 107 μ^δ on U , given the data δ .

108 **Theorem 1.** Assume that the potential $\Phi_\Gamma: U \times Y \rightarrow \mathbb{R}$ is μ_0 -measurable for $\delta \in Y$. Then
 109 the conditional distribution of \mathbf{y} given δ , denoted by $\mathbf{y}|\delta$, exists and is denoted by μ^δ . It is
 110 absolutely continuous with respect to μ_0 and its Radon-Nikodym derivative is given by

$$111 \quad (5) \quad \frac{d\mu^\delta}{d\mu_0}(\mathbf{y}) = \frac{1}{Z} \exp(-\Phi_\Gamma(\mathbf{y}, \delta)),$$

112 with $Z := \int_U \exp(-\Phi_\Gamma(\mathbf{y}, \delta)) \mu_0(d\mathbf{y}) > 0$.

113 *Proof.* See e.g. [11]. ■

114 The goal of computation is thus to approximate the posterior expectation $\mathbb{E}^{\mu^\delta}[\phi(q)] =$
 115 Z'/Z , where Z is given in Theorem 1 and

$$116 \quad (6) \quad Z' := \int_U \phi(q(\mathbf{y})) \exp(-\Phi_\Gamma(\mathbf{y}, \delta)) \mu_0(d\mathbf{y}).$$

117 The numerical approximation of $\mathbb{E}^{\mu^\delta}[\phi(q)]$ will consist of three parts:

- 118 (i) truncation of the infinite-parametric problem (1) to $s > 0$ parameters $\mathbf{y}^{(s)} = [y_1, \dots, y_s]^\top \in \blacksquare$
 119 $U^{(s)} := [-1/2, 1/2]^s$,
- 120 (ii) approximation of the solution $q^{(s)}(\mathbf{y}^{(s)})$ to the dimensionally truncated problem by a
 121 solution $q_h^{(s)}(\mathbf{y}^{(s)})$ obtained using a suitable discretization, and
- 122 (iii) approximation of the resulting s -dimensional integral over $\mathbf{y}^{(s)} \in U^{(s)}$.

123 For the latter, instead of resorting to Markov Chain Monte Carlo (MCMC) methods which
 124 converge at a (low) rate of $N^{-1/2}$ in the number of evaluations N of the forward model [32],
 125 we will adopt a direct, deterministic approach similar to [8, 40] and considered in the form
 126 used here for linear, affine-parametric problems in [13, 14]. To that end, we have to pro-
 127 vide parametric regularity estimates for the posterior measure, which will be provided in the
 128 following subsection.

129 **2.2. Parametric regularity of the posterior.** As stated above, it is well known that the
 130 system response q satisfies in relevant applications a parametric regularity estimate of the
 131 form (2). Therefore, we will take this estimate as a starting point for our analysis.

132 In view of Lemma 15 from the Appendix, we obtain the following straightforward result.

133 **Lemma 2.** Assume that the solution $q(\mathbf{y})$ to an operator equation of the form (1) satisfies
 134 (2) with $\gamma \in \ell^p(\mathbb{N})$ for $p < 1$. Then the system response q satisfies the decay estimate

$$135 \quad \|\partial_{\mathbf{y}}^\nu q(\mathbf{y})\|_{\mathcal{X}} \leq \frac{C}{1 - c_\lambda} \nu! c^{|\nu|} \tilde{\gamma}^\nu \quad \text{for all } \nu \in \mathcal{F}_\alpha.$$

136 where $\tilde{\gamma}_k := \gamma_k / \lambda_k$ with a positive sequence $\lambda \in \ell^1(\mathbb{N})$ and $c_\lambda := \|\lambda\|_{\ell^1(\mathbb{N})} < 1$.

137 This means that, given a sufficiently fast decay of the sequence γ , we can always replace the
 138 factor $|\nu|!$ by $\nu!$ due to modifying γ by an ℓ^1 -sequence, e.g. $\{k^{-1-\varepsilon}/\tilde{c}\}_k$ for arbitrary $\varepsilon > 0$
 139 and a normalization constant $\tilde{c} > 0$.

140 Now, let $\mathcal{O} \in \mathcal{L}(\mathcal{X}; \mathbb{R}^K)$ and let $\mathcal{G}(\mathbf{y})$ be defined as in (3). We want to analyze the behavior
 141 of the density

$$142 \quad \exp(-\Phi_\Gamma(\mathbf{y}, \delta)),$$

143 where the functional $\Phi_\Gamma(\mathbf{y}, \delta)$ is given by (4). Since \mathcal{O} is linear and bounded, we have

$$144 \quad (7) \quad \|\partial_{\mathbf{y}}^{\nu'}(\mathcal{O}g(\mathbf{y}))\|_{\mathbb{R}^K} = \|\mathcal{O}(\partial_{\mathbf{y}}^{\nu'}g(\mathbf{y}))\|_{\mathbb{R}^K} \leq \|\mathcal{O}\|_{\mathcal{L}(\mathcal{X}; \mathbb{R}^K)} C|\nu'|!c^{|\nu'|}\gamma^\nu \quad \text{for all } \nu \in \mathcal{F}_\alpha.$$

145 For the sake of simplicity let Γ be the identity matrix. Then, we start by considering

$$146 \quad \partial_{\mathbf{x}}^{\nu'} \exp\left(-\frac{1}{2}\mathbf{x}^\top \mathbf{x}\right).$$

147 In the univariate case, we know that

$$148 \quad \partial_x^{\nu'} \exp\left(-\frac{1}{2}x^2\right) = (-1)^{\nu'} \exp\left(-\frac{1}{2}x^2\right) H_{\nu'}(x),$$

149 where $H_{\nu'}$ is the probabilists' Hermite polynomial of degree ν' . By a tensor product argument,
150 we obtain

$$151 \quad \partial_{\mathbf{x}}^{\nu'} \exp\left(-\frac{1}{2}\mathbf{x}^\top \mathbf{x}\right) = (-1)^{|\nu'|} \exp\left(-\frac{1}{2}\mathbf{x}^\top \mathbf{x}\right) H_{\nu'}(\mathbf{x}).$$

152 Herein, the tensor product Hermite polynomial is given by

$$153 \quad H_{\nu'}(\mathbf{x}) := H_{\nu'_1}(x_1) \cdots H_{\nu'_K}(x_K).$$

154 Since the Hermite polynomials satisfy

$$155 \quad |H_{\nu'}(x)| \leq c_H \exp\left(\frac{x^2}{2}\right) \sqrt{\nu'!} \quad \text{with } c_H := 1.0685,$$

156 cp. [1], we have the following bound on the multivariate squared exponential function

$$157 \quad \left| \partial_{\mathbf{x}}^{\nu'} \exp\left(-\frac{1}{2}\mathbf{x}^\top \mathbf{x}\right) \right| \leq c_H^K \sqrt{\nu'!}.$$

158 Now, consider the affine transform $\mathbf{x} \mapsto \Gamma^{-1/2}(\delta - \mathbf{x})$, then we achieve the bound

$$159 \quad \left| \partial_{\mathbf{x}}^{\nu'} \exp\left(-\frac{1}{2}(\delta - \mathbf{x})^\top \Gamma^{-1}(\delta - \mathbf{x})\right) \right| \leq c_H^K \sqrt{\nu'!} \|\Gamma\|_2^{-\frac{|\nu'|}{2}}.$$

160 In particular, this implies that

$$161 \quad \Psi(\mathbf{x}) := \exp\left(-1/2(\delta - \mathbf{x})^\top \Gamma^{-1}(\delta - \mathbf{x})\right)$$

162 is an entire function on \mathbb{R}^K . We make use of the following result from [10].

163 **Theorem 3.** *Let $f(\mathbf{x}): \mathbb{R}^K \rightarrow \mathbb{R}$ be an entire function and $g^{(i)} \in C^\alpha(U^{(s)})$ for $i = 1, \dots, K$.
164 Then, the derivatives of $h(\mathbf{y}) := f(g^{(1)}(\mathbf{y}), \dots, g^{(K)}(\mathbf{y})) : U^{(s)} \rightarrow \mathbb{R}$ are given according to*

$$165 \quad (8) \quad \partial_{\mathbf{y}}^{\nu'} h(\mathbf{y}) = \nu'! \sum_{1 \leq |\nu'|} \frac{\partial_{\mathbf{x}}^{\nu'} f(\mathbf{x})|_{\mathbf{x}=\mathbf{0}}}{\nu'!} \sum_{s(\nu, \nu')} \prod_{i=1}^K \prod_{j=1}^{\nu'_i} \frac{\partial_{\mathbf{y}}^{\mu_j^{(i)}} g^{(i)}(\mathbf{y})}{\mu_j^{(i)}!} \quad \text{for all } \nu \in \mathcal{F}_\alpha.$$

166 Herein, the set $s(\nu, \nu')$ is defined as

$$167 \quad s(\nu, \nu') := \left\{ \left(\mu_1^{(1)}, \dots, \mu_{\nu'_1}^{(1)}, \dots, \mu_1^{(K)}, \dots, \mu_{\nu'_K}^{(K)} \right) : \mu_j^{(i)} \in \mathbb{N}^s \text{ and } \sum_{i=1}^K \sum_{j=1}^{\nu'_i} \mu_j^{(i)} = \nu \right\}.$$

168 *Proof.* See [10] for a proof of this statement. ■

169 Combining this estimate with the bound (7), gives the main result of this section.

170 **Theorem 4.** *Given that $\gamma \in \ell^p(\mathbb{N})$ for $p < 1/2$, the derivatives of $\exp(-\Phi_\Gamma(\mathbf{y}, \delta))$ can be*
 171 *bounded according to*

$$172 \quad \left| \partial_{\mathbf{y}}^\nu \exp(-\Phi_\Gamma(\mathbf{y}, \delta)) \right| \leq C(\Gamma, \boldsymbol{\lambda}, \mathcal{O})^K |\boldsymbol{\nu}|! (2c)^{|\boldsymbol{\nu}|} \tilde{\gamma}^\nu \quad \text{for all } \boldsymbol{\nu} \in \mathcal{F}_\alpha,$$

173 where $\tilde{\gamma}_k := \gamma_k/\lambda_k$ with a positive sequence $\boldsymbol{\lambda} \in \ell^1(\mathbb{N})$, $c_\lambda := \|\boldsymbol{\lambda}\|_{\ell^1(\mathbb{N})} < 1$, and $C(\Gamma, \boldsymbol{\lambda}, \mathcal{O}) > 0$
 174 is a constant.

175 *Proof.* From Lemma 2 and estimate (7), we derive that

$$176 \quad \left\| \partial_{\mathbf{y}}^\nu \mathcal{G}(\mathbf{y}) \right\|_{\mathbb{R}^K} \leq C(\boldsymbol{\lambda}, \mathcal{O}) \boldsymbol{\nu}! c^{|\boldsymbol{\nu}|} \tilde{\gamma}^\nu \quad \text{for all } \boldsymbol{\nu} \in \mathcal{F}_\alpha,$$

177 where $C(\boldsymbol{\lambda}, \mathcal{O}) := C\|\mathcal{O}\|_{\mathcal{L}(\mathcal{X}; \mathbb{R}^K)}/(1 - c_\lambda)$.

178 Now, the application of Theorem 3 gives us, cp. (8),

$$179 \quad \partial_{\mathbf{y}}^\nu \exp(-\Phi_\Gamma(\mathbf{y}, \delta)) = \boldsymbol{\nu}! \sum_{1 \leq |\boldsymbol{\nu}'|} \frac{\partial_{\mathbf{x}}^{\boldsymbol{\nu}'} \Psi(\mathbf{x})|_{\mathbf{x}=\mathbf{0}}}{\boldsymbol{\nu}'!} \sum_{s(\boldsymbol{\nu}, \boldsymbol{\nu}')} \prod_{i=1}^K \prod_{j=1}^{\nu'_i} \frac{\partial_{\mathbf{y}}^{\boldsymbol{\mu}_j^{(i)}} \mathcal{G}^{(i)}(\mathbf{y})}{\boldsymbol{\mu}_j^{(i)}!}.$$

180 We estimate

$$\begin{aligned} 181 \quad \left| \partial_{\mathbf{y}}^\nu \exp(-\Phi_\Gamma(\mathbf{y}, \delta)) \right| &\leq \boldsymbol{\nu}! \sum_{1 \leq |\boldsymbol{\nu}'|} \frac{|\partial_{\mathbf{x}}^{\boldsymbol{\nu}'} \Psi(\mathbf{x})|_{\mathbf{x}=\mathbf{0}}|}{\boldsymbol{\nu}'!} \sum_{s(\boldsymbol{\nu}, \boldsymbol{\nu}')} \prod_{i=1}^K \prod_{j=1}^{\nu'_i} \frac{|\partial_{\mathbf{y}}^{\boldsymbol{\mu}_j^{(i)}} \mathcal{G}^{(i)}(\mathbf{y})|}{\boldsymbol{\mu}_j^{(i)}!} \\ 182 \quad &\leq \boldsymbol{\nu}! \sum_{1 \leq |\boldsymbol{\nu}'|} \frac{c_H^K \|\Gamma\|_2^{-|\boldsymbol{\nu}'|}}{\sqrt{\boldsymbol{\nu}'!}} \sum_{s(\boldsymbol{\nu}, \boldsymbol{\nu}')} \prod_{i=1}^K \prod_{j=1}^{\nu'_i} \frac{C(\boldsymbol{\nu}, \mathcal{O}) \boldsymbol{\mu}_j^{(i)}! c^{|\boldsymbol{\mu}_j^{(i)}|} \tilde{\gamma}^{\boldsymbol{\mu}_j^{(i)}}}{\boldsymbol{\mu}_j^{(i)}!} \\ 183 \quad &\leq \boldsymbol{\nu}! c^{|\boldsymbol{\nu}|} \tilde{\gamma}^\nu \sum_{1 \leq |\boldsymbol{\nu}'|} \frac{c_H^K \|\Gamma\|_2^{-|\boldsymbol{\nu}'|}}{\sqrt{\boldsymbol{\nu}'!}} C(\boldsymbol{\nu}, \mathcal{O})^{|\boldsymbol{\nu}'|} \sum_{s(\boldsymbol{\nu}, \boldsymbol{\nu}')} 1. \end{aligned}$$

185 Thus, it remains to estimate the cardinality of the set $s(\boldsymbol{\nu}, \boldsymbol{\nu}')$. The number of weak integer
 186 compositions for ν_k of length $|\boldsymbol{\nu}'|$ is given according to, see e.g. [29],

$$187 \quad \left| \left\{ (\mu_1, \dots, \mu_{|\boldsymbol{\nu}'|}) : \mu_i \in \mathbb{N} \text{ and } \mu_1 + \dots + \mu_{|\boldsymbol{\nu}'|} = \nu_k \right\} \right| = \binom{\nu_k + |\boldsymbol{\nu}'| - 1}{|\boldsymbol{\nu}'| - 1}.$$

188 By multiplying the number of possible compositions in each component, we can determine
 189 the cardinality of the set $s(\boldsymbol{\nu}, \boldsymbol{\nu}')$ by

$$190 \quad |s(\boldsymbol{\nu}, \boldsymbol{\nu}')| = \prod_{k=1}^s \binom{\nu_k + |\boldsymbol{\nu}'| - 1}{|\boldsymbol{\nu}'| - 1}.$$

191 We may bound this cardinality due to the estimate obtained by Lemma 17, i.e.

$$192 \quad \prod_{k=1}^s \binom{\nu_k + |\boldsymbol{\nu}'| - 1}{|\boldsymbol{\nu}'| - 1} \leq \frac{|\boldsymbol{\nu}'|!}{\boldsymbol{\nu}'!} \binom{|\boldsymbol{\nu}'| + |\boldsymbol{\nu}'| - 1}{|\boldsymbol{\nu}'| - 1} \leq \frac{|\boldsymbol{\nu}'|!}{\boldsymbol{\nu}'!} 2^{|\boldsymbol{\nu}'| + |\boldsymbol{\nu}'|}.$$

193 Therefore, we arrive at

$$194 \quad \left| \partial_{\mathbf{y}}^{\nu'} \exp(-\Phi_{\Gamma}(\mathbf{y}, \delta)) \right| \leq |\nu'|! (2c)^{|\nu'|} \tilde{\gamma}^{\nu'} \sum_{1 \leq |\nu'|} \frac{c_H^K \|\Gamma\|_2^{-\frac{|\nu'|}{2}}}{\sqrt{\nu'!}} (2C(\boldsymbol{\lambda}, \mathcal{O}))^{|\nu'|}.$$

195 Obviously, the series

$$196 \quad \sum_{\nu'_i=0}^{\infty} \frac{c_H \|\Gamma\|_2^{-\frac{\nu'_i}{2}}}{\sqrt{\nu'_i!}} (2C(\boldsymbol{\lambda}, \mathcal{O}))^{\nu'_i}$$

197 is absolutely convergent with respect to each particular direction ν'_i . Let its limit be $C(\Gamma, \boldsymbol{\lambda}, \mathcal{O})$.
 198 Hence, by taking the product of this limit with respect to the K components of ν' , we arrive
 199 at the assertion. ■

200 3. Forward model.

201 **3.1. The domain mapping method.** In this section, we formulate the diffusion problem
 202 on random domains as is has been addressed in [27]. To that end, let $(\Omega, \mathcal{A}, \mathbb{P})$ denote a
 203 complete and separable probability space with σ -algebra \mathcal{A} and probability measure \mathbb{P} . Here,
 204 complete means that \mathcal{A} contains all \mathbb{P} -null sets. For a given Banach space \mathcal{X} , we introduce
 205 the Bochner space $L_{\mathbb{P}}^p(\Omega; \mathcal{X})$, $1 \leq p \leq \infty$, which consists of all equivalence classes of strongly
 206 measurable functions $v: \Omega \rightarrow \mathcal{X}$ whose norm

$$207 \quad \|v\|_{L_{\mathbb{P}}^p(\Omega; \mathcal{X})} := \begin{cases} \left(\int_{\Omega} \|v(\cdot, \omega)\|_{\mathcal{X}}^p d\mathbb{P}(\omega) \right)^{1/p}, & p < \infty \\ \text{ess sup}_{\omega \in \Omega} \|v(\cdot, \omega)\|_{\mathcal{X}}, & p = \infty \end{cases}$$

208 is finite. If $p = 2$ and \mathcal{X} is a separable Hilbert space, then the Bochner space $L_{\mathbb{P}}^p(\Omega; \mathcal{X})$ is
 209 isomorphic to the tensor product space $L_{\mathbb{P}}^2(\Omega) \otimes \mathcal{X}$. For more details on Bochner spaces, we
 210 refer the reader to [31].

211 Now, given a random domain $D(\omega) \subset \mathbb{R}^d$ for $d = 2, 3$, we assume the existence of a
 212 reference domain $D_0 \subset \mathbb{R}^d$ and of a *uniform C^1 -diffeomorphism* $\mathbf{V}: \overline{D_0} \times \Omega \rightarrow \mathbb{R}^d$, i.e.

$$213 \quad (9) \quad \|\mathbf{V}(\omega)\|_{C^1(\overline{D_0}; \mathbb{R}^d)}, \|\mathbf{V}^{-1}(\omega)\|_{C^1(\overline{D_0}; \mathbb{R}^d)} \leq C_{\text{uni}} \quad \text{for } \mathbb{P}\text{-a.e. } \omega \in \Omega,$$

214 such that $D(\omega)$ is implicitly given by the relation

$$215 \quad D(\omega) = \mathbf{V}(D_0, \omega).$$

216 Particularly, since $\mathbf{V} \in L^{\infty}(\Omega; C^1(\overline{D_0})) \subset L^2(\Omega; C^1(\overline{D_0}))$, the vector field \mathbf{V} exhibits a
 217 Karhunen-Loève expansion of the form

$$218 \quad \mathbf{V}(\mathbf{x}, \omega) = \mathbb{E}[\mathbf{V}](\mathbf{x}) + \sum_{k=1}^{\infty} \mathbf{V}_k(\mathbf{x}) Y_k(\omega).$$

219 The anisotropy which is induced by the spatial parts $\{\mathbf{V}_k\}_k$, describing the fluctuations around
 220 the nominal value $\mathbb{E}[\mathbf{V}](\mathbf{x})$, is encoded by

$$221 \quad (10) \quad \gamma_k := \|\mathbf{V}_k\|_{W^{1,\infty}(D_0; \mathbb{R}^d)}.$$

222 For our modeling, we shall also make the following common assumptions.

223 **Assumption 5.**

- 224 (i) The random variables $\{Y_k\}_k$ take values in $[-1/2, 1/2]$.
 225 (ii) The random variables $\{Y_k\}_k$ are independent and identically distributed.
 226 (iii) The sequence $\{\gamma_k\}_k$ is at least in $\ell^1(\mathbb{N})$.

227 By an appropriate reparametrization, we can achieve that $\mathbb{E}[\mathbf{V}](\mathbf{x}) = \mathbf{x}$. Moreover, if we
 228 identify the random variables by their image $\mathbf{y} \in U = [-1/2, 1/2]^{\mathbb{N}}$, we end up with the
 229 representation

$$230 \quad (11) \quad \mathbf{V}(\mathbf{x}, \mathbf{y}) = \mathbf{x} + \sum_{k=1}^{\infty} \mathbf{V}_k(\mathbf{x}) y_k.$$

231 The Jacobian of \mathbf{V} with respect to the spatial variable \mathbf{x} is thus given by

$$232 \quad \mathbf{J}(\mathbf{x}, \mathbf{y}) = \mathbf{I} + \sum_{k=1}^{\infty} \mathbf{V}'_k(\mathbf{x}) y_k.$$

233 Introducing the parametric domains $D(\mathbf{y}) := \mathbf{V}(D_0, \mathbf{y})$, the forward problem which we con-
 234 sider here becomes:

235 Find $q \in H^1(D(\mathbf{y}))$ such that

$$236 \quad (12) \quad \begin{aligned} -\Delta q(\mathbf{y}) &= 0 && \text{in } D(\mathbf{y}), \\ q(\mathbf{y}) &= g && \text{on } \partial D(\mathbf{y}). \end{aligned}$$

237 To guarantee the solvability of the model problem for every realization of the parameter $\mathbf{y} \in U$,
 238 it is reasonable to postulate that the Dirichlet data g are defined on the entire hold-all domain
 239 $\mathcal{D} := \cup_{\mathbf{y} \in U} D(\mathbf{y})$. Moreover, to derive regularity results that are independent of the parameter
 240 dimension, it is necessary that g is an analytic function see [27]. Nevertheless, in view of (2),
 241 we shall weaken this estimate and only require that there holds

$$242 \quad (13) \quad \|\partial_{\mathbf{y}}^{\nu}(\Delta g \circ \mathbf{V})(\mathbf{y})\|_{L^{\infty}(D_0)} \leq C |\nu|! c^{|\nu|} \gamma^{\nu} \quad \text{for all } \nu \in \mathcal{F}_{\alpha}$$

243 for some constants $C, c > 0$. Thus, it would be sufficient to postulate $\Delta g \in C^{|\alpha|}(D(\mathbf{y}))$ for
 244 all $\mathbf{y} \in U$. Hence, we can reformulate the problem by making the ansatz

$$245 \quad q(\mathbf{y}) = q_0(\mathbf{y}) + g.$$

246 This results in:

247 Find $q_0 \in H_0^1(D(\mathbf{y}))$ such that

$$248 \quad \begin{aligned} -\Delta q_0(\mathbf{y}) &= \Delta g && \text{in } D(\mathbf{y}), \\ q_0(\mathbf{y}) &= 0 && \text{on } \partial D(\mathbf{y}). \end{aligned}$$

249 From this, we can easily derive the variational formulation:

250 Find $q_0 \in H_0^1(D(\mathbf{y}))$ such that there holds for all $v \in H_0^1(D(\mathbf{y}))$ that

$$251 \quad \int_{D(\mathbf{y})} \nabla q_0(\mathbf{y}) \nabla v \, d\mathbf{x} = \int_{D(\mathbf{y})} (\Delta g)v \, d\mathbf{x}.$$

252 Now, defining

$$253 \quad (14) \quad \mathbf{A}(\mathbf{x}, \mathbf{y}) := [\mathbf{J}^\top \mathbf{J}]^{-1}(\mathbf{x}, \mathbf{y}) \det \mathbf{J}(\mathbf{x}, \mathbf{y}) \quad \text{and} \quad \hat{f}(\mathbf{x}, \mathbf{y}) := (\Delta g)(\mathbf{V}(\mathbf{x}, \mathbf{y})) \det \mathbf{J}(\mathbf{x}, \mathbf{y}),$$

254 we arrive at the variational formulation on the reference domain D_0 , which reads:

255 Find $\hat{q}_0 \in H_0^1(D_0)$ such that there holds for all $v \in H_0^1(D_0)$ that

$$256 \quad \int_{D_0} \mathbf{A}(\mathbf{y}) \nabla \hat{q}_0(\mathbf{y}) \nabla v \, d\mathbf{x} = \int_{D_0} \hat{f}(\mathbf{y})v \, d\mathbf{x}.$$

257 We note that $q_0(\mathbf{y}) = \hat{q}_0 \circ \mathbf{V}^{-1}(\mathbf{y})$ and for all $\mathbf{y} \in U$, we derive

$$258 \quad (15) \quad \|\partial_{\mathbf{y}}^\nu \hat{q}_0(\mathbf{y})\|_{H_0^1(D_0)} \leq C |\nu|! c^{|\nu|} \gamma^\nu \quad \text{for all } \nu \in \mathcal{F}_\alpha,$$

259 for a sequence $\gamma \in \ell^p(\mathbb{N})$ for some $p < 1$, given here by (10), and some constants $C, c > 0$,
 260 see [27] for the details. A regularity estimate similar to (15) particularly accounts for the
 261 system response \hat{q} of the forward problem (12) transported to D_0 , which is a straightforward
 262 consequence of the smoothness requirements (13) in the Dirichlet data and the application of
 263 the Faà di Bruno's formula.

264 **3.2. Dimension truncation.** In this subsection, we shall supplement the analysis pre-
 265 sented in [27] by discussing the error of dimension truncation. As a starting point, we con-
 266 sider the general representation (11) of the vector field. We refer to s as the *truncation*
 267 *dimension* or *parametric dimension* of the problem. By considering now sequences of the
 268 form $\mathbf{y} = \{y_1, \dots, y_s, 0, \dots\}$, the following lemma is immediate.

269 **Lemma 6.** *Let the Jacobian of the truncated expansion of the vector field \mathbf{V} be defined as*

$$270 \quad \mathbf{J}^{(s)}(\mathbf{x}, \mathbf{y}) := \mathbf{I} + \sum_{k=1}^s \mathbf{V}'_k(\mathbf{x}) y_k \quad \text{and set} \quad \varepsilon_\gamma^{(s)} := \sum_{k=s+1}^{\infty} \gamma_k.$$

271 *Then, there holds*

$$272 \quad \frac{1}{C_{\text{uni}}} \leq \|\mathbf{J}^{(s)}(\mathbf{y})\|_{L^\infty(D_0; \mathbb{R}^{d \times d})} \leq C_{\text{uni}}$$

273 *with the same constant as in (9), where the bounds hold uniformly in s .*

274 Given sufficient summability of the sequence γ , we obtain the following bound on the
 275 truncation error.

276 **Lemma 7.** *Let $\varepsilon_\gamma^{(s)}$ be defined as in Lemma 6. Assume that the sequence γ is nonincreasing,*
 277 *$\gamma_1 \geq \gamma_2 \dots$, and assume additionally that there exists $p \in (0, 1)$ such that $\gamma \in \ell^p(\mathbb{N})$. Then,*

$$278 \quad (16) \quad \varepsilon_\gamma^{(s)} \leq C(p, \gamma) s^{-\theta(1/p-1)},$$

279 *with $C(p, \gamma) = \min((1/p - 1)^{-1}, 1) \|\gamma\|_{\ell^p}$ and $\theta = 1$ in general. If $\int_{-1/2}^{1/2} y_j \mu_0(dy_j) = 0$ for all*
 280 *$j \in \mathbb{N}$, we have $\theta = 2$.*

281 *Proof.* See e.g. [15, Thm. 2.6] and [36]. ■

282 Now, we consider the impact of truncation on $\det \mathbf{J}(\mathbf{y})$ and $[\mathbf{J}^\top \mathbf{J}](\mathbf{y})$ separately.

283 **Lemma 8.** *The determinant of the truncated Jacobian satisfies the estimate*

$$284 \quad \left| \det \mathbf{J}(\mathbf{y}) - \det \mathbf{J}^{(s)}(\mathbf{y}) \right| \leq d C_{\text{uni}}^{d-1} \varepsilon_\gamma^{(s)}.$$

285 *Proof.* For the determinant function and two matrices $\mathbf{M}, \mathbf{M}' \in \mathbb{R}^{d \times d}$ with bounded
286 columns $\|\mathbf{M}_i\|_2, \|\mathbf{M}'_i\|_2 \leq c$ for $i = 1, \dots, d$ and $c > 0$, we know

$$287 \quad \left| \det \mathbf{M} - \det \mathbf{M}' \right| \leq d c^{d-1} \|\mathbf{M} - \mathbf{M}'\|_2.$$

288 Obviously, we can bound each column of \mathbf{J} and $\mathbf{J}^{(s)}$ by C_{uni} . Therefore, we arrive at

$$289 \quad \left| \det \mathbf{J}(\mathbf{y}) - \det \mathbf{J}^{(s)}(\mathbf{y}) \right| \leq d C_{\text{uni}}^{d-1} \|\mathbf{J}(\mathbf{y}) - \mathbf{J}^{(s)}(\mathbf{y})\|_2 \leq d C_{\text{uni}}^{d-1} \varepsilon_\gamma^{(s)}. \quad \blacksquare$$

290 **Lemma 9.** *For the truncation of the matrix $[\mathbf{J}^\top \mathbf{J}]^{-1}(\mathbf{y})$, there holds the estimate*

$$291 \quad \left\| [\mathbf{J}^\top \mathbf{J}]^{-1}(\mathbf{y}) - [(\mathbf{J}^{(s)})^\top \mathbf{J}^{(s)}]^{-1}(\mathbf{y}) \right\|_{L^\infty(D_0; \mathbb{R}^{d \times d})} \leq \frac{2}{C_{\text{uni}}} \varepsilon_\gamma^{(s)} + O(\varepsilon_\gamma^{(s)})^2.$$

292 *Proof.* A straightforward calculation yields

$$293 \quad \left\| [\mathbf{J}^\top \mathbf{J}](\mathbf{y}) - [(\mathbf{J}^{(s)})^\top \mathbf{J}^{(s)}](\mathbf{y}) \right\|_{L^\infty(D_0; \mathbb{R}^{d \times d})} \leq 2 C_{\text{uni}} \varepsilon_\gamma^{(s)} + O(\varepsilon_\gamma^{(s)})^2.$$

294 Therefore, a first order Taylor expansion gives us, see e.g. [30],

$$\begin{aligned} 295 \quad & \left\| [\mathbf{J}^\top \mathbf{J}]^{-1}(\mathbf{y}) - [(\mathbf{J}^{(s)})^\top \mathbf{J}^{(s)}]^{-1}(\mathbf{y}) \right\|_{L^\infty(D_0; \mathbb{R}^{d \times d})} \\ 296 \quad & \leq 2 C_{\text{uni}} \varepsilon_\gamma^{(s)} \left\| [\mathbf{J}^\top \mathbf{J}](\mathbf{y}) \right\|_{L^\infty(D_0; \mathbb{R}^{d \times d})} \left\| [\mathbf{J}^\top \mathbf{J}]^{-1}(\mathbf{y}) \right\|_{L^\infty(D_0; \mathbb{R}^{d \times d})}^2 + O(\varepsilon_\gamma^{(s)})^2 \\ 297 \quad & \leq 2 \frac{C_{\text{uni}}}{C_{\text{uni}}^2} \varepsilon_\gamma^{(s)} + O(\varepsilon_\gamma^{(s)})^2, \\ 298 \end{aligned}$$

299 where we applied the bounds

$$300 \quad \left\| [\mathbf{J}^\top \mathbf{J}]^{-1}(\mathbf{y}) \right\|_{L^\infty(D_0; \mathbb{R}^{d \times d})} \leq 1/C_{\text{uni}}^2 \quad \text{and} \quad \left\| [\mathbf{J}^\top \mathbf{J}](\mathbf{y}) \right\|_{L^\infty(D_0; \mathbb{R}^{d \times d})} \leq C_{\text{uni}}^2. \quad \blacksquare$$

301 Having these lemmata at hand, we can bound the truncation error in the diffusion matrix
302 and in the right hand side.

303 **Theorem 10.** *The truncation errors in the diffusion matrix and in the right hand side*
304 *satisfy the error estimates*

$$305 \quad \left\| \mathbf{A}(\mathbf{y}) - \mathbf{A}^{(s)}(\mathbf{y}) \right\|_{L^\infty(D_0; \mathbb{R}^{d \times d})} \leq (2 + d) C_{\text{uni}}^{d-1} \varepsilon_\gamma^{(s)} + O(\varepsilon_\gamma^{(s)})^2$$

306 and

$$307 \quad \left\| \hat{f}(\mathbf{y}) - \hat{f}^{(s)}(\mathbf{y}) \right\|_{L^\infty(D_0)} \leq (d + C_{\text{uni}}) \|\Delta g\|_{W^{1, \infty}} C_{\text{uni}}^{d-1} \varepsilon_\gamma^{(s)}.$$

308 *In these estimates, the quantities $\mathbf{A}^{(s)}(\mathbf{y})$ and $\hat{f}^{(s)}(\mathbf{y})$ are simply obtained by replacing \mathbf{J} in*
309 *(14) by $\mathbf{J}^{(s)}$.*

310 *Proof.* By the application of the triangle inequality, we can now simply bound the truncation error for the diffusion matrix according to

$$\begin{aligned}
312 & \quad \|\mathbf{A}(\mathbf{y}) - \mathbf{A}^{(s)}(\mathbf{y})\|_{L^\infty(D_0; \mathbb{R}^{d \times d})} \\
313 & \quad \leq \left\| \mathbf{A}(\mathbf{y}) - [\mathbf{J}^\top \mathbf{J}]^{-1}(\mathbf{y}) \det \mathbf{J}^{(s)}(\mathbf{y}) \right\|_{L^\infty(D_0; \mathbb{R}^{d \times d})} \\
314 & \quad + \left\| [\mathbf{J}^\top \mathbf{J}]^{-1}(\mathbf{y}) \det \mathbf{J}^{(s)}(\mathbf{y}) - \mathbf{A}^{(s)}(\mathbf{y}) \right\|_{L^\infty(D_0; \mathbb{R}^{d \times d})} \\
315 & \quad \leq \frac{1}{C_{\text{uni}}^2} d C_{\text{uni}}^{d-1} \varepsilon_\gamma^{(s)} + \frac{2}{C_{\text{uni}}} \varepsilon_\gamma^{(s)} C_{\text{uni}}^d + O(\varepsilon_\gamma^{(s)})^2 \\
316 & \quad \leq (2 + d) C_{\text{uni}}^{d-1} \varepsilon_\gamma^{(s)} + O(\varepsilon_\gamma^{(s)})^2.
\end{aligned}$$

318 where we applied the bounds

$$319 \quad \left\| [\mathbf{J}^\top \mathbf{J}]^{-1}(\mathbf{y}) \right\|_{L^\infty(D_0; \mathbb{R}^{d \times d})} \leq \frac{1}{C_{\text{uni}}^2} \quad \text{and} \quad |\det \mathbf{J}^{(s)}(\mathbf{y})| \leq C_{\text{uni}}^d.$$

320 In complete analogy, we can bound the truncation error in the right hand side according
321 to

$$\begin{aligned}
& \quad \|\hat{f}(\mathbf{y}) - \hat{f}^{(s)}(\mathbf{y})\|_{L^\infty(D_0)} \\
& \quad \leq \left\| \hat{f}(\mathbf{y}) - (\Delta g \circ \mathbf{V})(\mathbf{y}) \det \mathbf{J}^{(s)}(\mathbf{y}) \right\|_{L^\infty(D_0)} \\
& \quad \quad + \left\| (\Delta g \circ \mathbf{V})(\mathbf{y}) \det \mathbf{J}^{(s)}(\mathbf{y}) - \hat{f}^{(s)}(\mathbf{y}) \right\|_{L^\infty(D_0)} \\
& \quad \leq \|\Delta g\|_{L^\infty(D)} d C_{\text{uni}}^{d-1} \varepsilon_\gamma^{(s)} + \|\Delta g\|_{W^{1,\infty}(D)} \varepsilon_\gamma^{(s)} C_{\text{uni}}^d \\
322 & \quad \leq (d + C_{\text{uni}}) \|\Delta g\|_{W^{1,\infty}(D)} C_{\text{uni}}^{d-1} \varepsilon_\gamma^{(s)}. \quad \blacksquare
\end{aligned}$$

323 From Lemma 6, we infer that the diffusion matrix $\mathbf{A}^{(s)}(\mathbf{y})$ is always elliptic, i.e. there
324 holds

$$325 \quad \mathbf{z}^\top \mathbf{A}^{(s)}(\mathbf{x}, \mathbf{y}) \mathbf{z} \geq a_{\min} > 0 \quad \text{for all } \mathbf{z} \in \mathbb{R}^d \text{ uniformly in } s.$$

326 Thus, let $\hat{q}_0^{(s)} \in H_0^1(D_0)$ be the unique solution of the variational formulation

$$327 \quad \int_{D_0} \mathbf{A}^{(s)}(\mathbf{y}) \nabla \hat{q}_0^{(s)} \nabla v \, d\mathbf{x} = \int_{D_0} \hat{f}^{(s)}(\mathbf{y}) v \, d\mathbf{x}.$$

328 Having the impact of truncating the Jacobian on the diffusion coefficient and the right hand
329 side at hand, we may now bound the respective error of the solution in analogy to Strang's
330 lemma.

331 **Theorem 11.** *There holds for a constant $C > 0$, which depends on the domain D_0 , the
332 spatial dimension d as well as $\|\Delta g\|_{W^{1,\infty}}$ and C_{uni} , the error estimate*

$$333 \quad \left\| (\hat{q}_0 - \hat{q}_0^{(s)})(\mathbf{y}) \right\|_{H_0^1(D_0)} \leq \frac{C}{a_{\min}} (1 + \|\hat{q}_0(\mathbf{y})\|_{H_0^1(D_0)}) \varepsilon_\gamma^{(s)} + O(\varepsilon_\gamma^{(s)})^2.$$

334 *Proof.* Making use of the ellipticity of the bilinear form induced by $\mathbf{A}^{(s)}(\mathbf{y})$, we have

$$\begin{aligned}
335 \quad & a_{\min} \|(\hat{q}_0 - \hat{q}_0^{(s)})(\mathbf{y})\|_{H_0^1(D_0)}^2 \\
336 \quad & \leq \int_{D_0} \mathbf{A}^{(s)}(\mathbf{y}) \nabla(\hat{q}_0 - \hat{q}_0^{(s)})(\mathbf{y}) \nabla(\hat{q}_0 - \hat{q}_0^{(s)})(\mathbf{y}) \, d\mathbf{x} \\
337 \quad & = \int_{D_0} \mathbf{A}^{(s)}(\mathbf{y}) \nabla \hat{q}_0(\mathbf{y}) \nabla(\hat{q}_0 - \hat{q}_0^{(s)})(\mathbf{y}) \, d\mathbf{x} - \int_{D_0} \hat{f}^{(s)}(\mathbf{y}) (\hat{q}_0 - \hat{q}_0^{(s)})(\mathbf{y}) \, d\mathbf{x} \\
338 \quad & = \int_{D_0} (\mathbf{A}^{(s)} - \mathbf{A})(\mathbf{y}) \nabla \hat{q}_0(\mathbf{y}) \nabla(\hat{q}_0 - \hat{q}_0^{(s)})(\mathbf{y}) \, d\mathbf{x} \\
339 \quad & \quad - \int_{D_0} (\hat{f}^{(s)} - \hat{f})(\mathbf{y}) (\hat{q}_0 - \hat{q}_0^{(s)})(\mathbf{y}) \, d\mathbf{x} \\
340 \quad & \leq \|\mathbf{A}(\mathbf{y}) - \mathbf{A}^{(s)}(\mathbf{y})\|_{L^\infty(D_0; \mathbb{R}^{d \times d})} \|(\hat{q}_0 - \hat{q}_0^{(s)})(\mathbf{y})\|_{H_0^1(D_0)} \|\hat{q}_0(\mathbf{y})\|_{H_0^1(D_0)} \\
341 \quad & \quad + \|\hat{f}(\mathbf{y}) - \hat{f}^{(s)}(\mathbf{y})\|_{H^{-1}(D_0)} \|(\hat{q}_0 - \hat{q}_0^{(s)})(\mathbf{y})\|_{H_0^1(D_0)}. \\
342
\end{aligned}$$

343 Now, we exploit

$$344 \quad \|\hat{f}(\mathbf{y}) - \hat{f}^{(s)}(\mathbf{y})\|_{H^{-1}(D_0)} \leq c_P \sqrt{|D_0|} \|\hat{f}(\mathbf{y}) - \hat{f}^{(s)}(\mathbf{y})\|_{L^\infty(D_0)},$$

345 where $c_P > 0$ is the Poincaré constant for D_0 and $|D_0|$ is the Lebesgue measure of D_0 . Then,
346 simplifying this expression and inserting the bounds from Theorem 10 results in

$$\begin{aligned}
347 \quad & \|(\hat{q}_0 - \hat{q}_0^{(s)})(\mathbf{y})\|_{H_0^1(D_0)} \leq \frac{1}{a_{\min}} (2 + d) C_{\text{uni}}^{d-1} \varepsilon_\gamma^{(s)} \|\hat{q}_0(\mathbf{y})\|_{H_0^1(D_0)} + O(\varepsilon_\gamma^{(s)})^2 \\
& \quad + \frac{1}{a_{\min}} c_P \sqrt{|D_0|} (d + C_{\text{uni}}) \|\Delta g\|_{W^{1,\infty}} C_{\text{uni}}^{d-1} \varepsilon_\gamma^{(s)}. \quad \blacksquare
\end{aligned}$$

348 **4. Electrical Impedance Tomography.** Now, let $\mathcal{D} \subset \mathbb{R}^2$ denote a simply-connected and
349 convex domain with Lipschitz continuous boundary $\Sigma := \partial\mathcal{D}$. Inside the domain, we suppose
350 that there exists a simply connected subdomain $S \Subset \mathcal{D}$ with boundary $\Gamma := \partial S$. The boundary
351 Γ shall be of co-dimension 1 and, thus, separate the interior domain S and the outer domain
352 \mathcal{D} . The resulting, annular domain $\mathcal{D} \setminus \bar{S}$ shall be referred to as D .

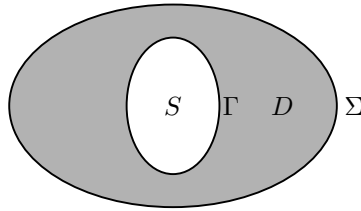


Figure 1: The domain D with inner and outer boundaries Γ and Σ , respectively, and the inclusion S .

353 A sketch of the situation can be found in Figure 1. The inner domain S models a material
 354 of constant conductivity that is significantly different from the (also constant) conductivity of
 355 the material in the annular domain D . We are interested in the identification of the inclusion
 356 S . To that end, for a given voltage distribution $g_D \in H^{1/2}(\Sigma)$, we measure the corresponding
 357 current distribution $g_N \in H^{-1/2}(\Sigma)$. This means that we are looking for a domain D which
 358 satisfies the overdetermined boundary value problem

$$\begin{aligned}
 & \Delta q = 0 \quad \text{in } D, \\
 & \gamma_{0,\Gamma}^{\text{int}} q = 0 \quad \text{on } \Gamma, \\
 & \gamma_{0,\Sigma}^{\text{int}} q = g_D \quad \text{on } \Sigma, \\
 & \gamma_{1,\Sigma}^{\text{int}} q = g_N \quad \text{on } \Sigma.
 \end{aligned}
 \tag{17}$$

360 Herein, the operators $\gamma_{0,\Gamma}^{\text{int}}$ and $\gamma_{0,\Sigma}^{\text{int}}$ denote the interior trace operators at Γ and Σ , re-
 361 spectively, whereas $\gamma_{1,\Sigma}^{\text{int}}$ is the co-normal derivative at Σ . Instead of successively solving this
 362 problem by an optimization procedure, as it has been done in e.g. [18], we will approach it here
 363 by means of Bayesian inversion. In this context, we assume that the measured Neumann data
 364 at Σ are subject to uncertainty and assume a prior distribution on the parameters describing
 365 the boundary. In order to quantify the resulting uncertainty inherent in this problem, we
 366 reformulate the associated forward problem in terms of an elliptic diffusion problem which is
 367 stated on a random domain.

368 Due to our lack of knowledge on the shape of the inclusion, we consider the interior
 369 domain to be random. This uncertainty is incorporated by assuming the interior boundary to
 370 be \mathbb{P} -a.s. star-shaped and modeling it according to

$$\Gamma(\omega) = \{ \mathbf{x} = \boldsymbol{\sigma}(t, \omega) \in \mathbb{R}^2 : \boldsymbol{\sigma}(t, \omega) = u(t, \omega) \mathbf{e}(t), t \in I \},
 \tag{18}$$

372 where $\boldsymbol{\sigma}(t, \omega)$ is a random field. Furthermore, let $\mathbf{e}(t) := [\cos(t), \sin(t)]^\top$ denote the radial
 373 direction and $I := [0, 2\pi]$ be the interval for the angle t . We note that with the techniques
 374 presented in the previous section it is possible to treat more general inclusions. Nevertheless,
 375 our particular choice facilitates a sensible definition of an expected shape. Additionally, the
 376 variance (or higher moments) of the parameters can be computed, yielding via (18) a confi-
 377 dence region for the inclusion. In accordance with [25], we define the boundary's mean and
 378 variance as

$$\begin{aligned}
 \mathbb{E}[\Gamma(\omega)] &= \{ \mathbf{x} \in \mathbb{R}^2 : \mathbf{x} = \mathbb{E}[u(t, \omega)] \mathbf{e}(t), t \in I \} \\
 \mathbb{V}[\Gamma(\omega)] &= \{ \mathbf{x} \in \mathbb{R}^2 : \mathbf{x} = \mathbb{V}[u(t, \omega)] \mathbf{e}(t), t \in I \}.
 \end{aligned}$$

382 To that end, the radial function $u(t, \omega) \geq \underline{c} > 0$ has to be in the Bochner space $L^2(\Omega; C_{\text{per}}^2(I))$,
 383 where $C_{\text{per}}^2(I)$ denotes the Banach space of periodic, twice continuously differentiable func-
 384 tions, i.e.

$$C_{\text{per}}^2(I) := \{ f \in C^2(I) : f^{(i)}(0) = f^{(i)}(2\pi), i = 0, 1, 2 \},$$

386 equipped with the norm

$$\|f\|_{C_{\text{per}}^2(I)} := \sum_{i=0}^2 \max_{x \in I} |f^{(i)}(x)|.$$

388 If $u(t, \omega)$ is described by its expectation

$$389 \quad \mathbb{E}[u](t) = \int_{\Omega} u(t, \omega) \, d\mathbb{P}(\omega)$$

390 and its covariance

$$391 \quad \text{Cov}[u](t, t') = \mathbb{E}[u(t, \omega)u(t', \omega)] = \int_{\Omega} u(t, \omega)u(t', \omega) \, d\mathbb{P}(\omega),$$

392 then we can represent it by its *Karhunen-Loève expansion*, cf. [37],

$$393 \quad u(t, \omega) = \mathbb{E}[u](t) + \sum_{k=1}^{\infty} u_k(t)Y_k(\omega).$$

394 Herein, the functions $\{u_k(\varphi)\}_k$ are scaled versions of the eigenfunctions of the Hilbert-Schmidt
 395 operator associated to $\text{Cov}[u](t, t')$. Common approaches to numerically recover the Karhunen-
 396 Loève expansion from these quantities are e.g. given in [26, 42]. By construction, the random
 397 variables $\{Y_k(\omega)\}_k$ in the Karhunen-Loève expansion are uncorrelated. For our modeling, we
 398 shall also impose the conditions of Assumption 5, where we modify the third condition as
 399 follows:

400 (iii)' The sequence $\{\hat{\gamma}_k\}_k := \{\|u_k\|_{W^{1,\infty}(0,2\pi)}\}_k$ is at least in $\ell^1(\mathbb{N})$.

401 The domain $D(\omega)$ shall now be identified by its boundaries $\Gamma(\omega)$ and Σ . Then, we face
 402 the following forward problem:

403 Find $q \in H^1(D(\omega))$ such that

$$404 \quad (19) \quad \begin{aligned} -\Delta q(\omega) &= 0 && \text{in } D(\omega), \\ q(\omega) &= g && \text{on } \partial D(\omega), \end{aligned}$$

405 where $g|_{\Gamma(\omega)} = 0$ and $g|_{\Sigma} = g_D$.

406 The parametric regularity may now be obtained as in the previous section. To that end,
 407 we cast the forward model into the framework of the domain mapping method as it has been
 408 done in [27] and employ the regularity results presented there. The boundary $\Gamma(\omega)$ in (18) is
 409 already parametrized with respect to the reference boundary $\Gamma_0 := \mathbb{E}[\Gamma]$. Hence, it is sensible
 410 to introduce the reference domain $D_0 \subset \mathbb{R}^2$ that is enclosed by the boundaries Γ_0 and Σ .

411 Thus, by a suitable extension, we can achieve that $\Gamma(\omega)$ is given by the application of a
 412 vector field $\mathbf{V}: \overline{D_0} \times \Omega \rightarrow \mathbb{R}^2$, i.e. $\Gamma(\omega) = \mathbf{V}(\Gamma_0, \omega)$. If Γ_0 is of class C^2 , a possibility to define
 413 \mathbf{V} is given as follows:

$$414 \quad (20) \quad \mathbf{V}(\mathbf{x}, \omega) := \mathbf{x} + \sum_{k=1}^{\infty} u_k(\arg P\mathbf{x}) \begin{bmatrix} \cos(\arg P\mathbf{x}) \\ \sin(\arg P\mathbf{x}) \end{bmatrix} B(\|\mathbf{x} - P\mathbf{x}\|_2)Y_k(\omega),$$

415 where $P\mathbf{x}$ is the orthogonal projection of \mathbf{x} onto Γ_0 and $B: [0, \infty) \rightarrow [0, 1]$ is a smooth blending
 416 function with $B(0) = 1$ and $B(t) = 0$ for all $t \geq c$ for some constant $c \in (0, \infty)$. Notice that
 417 if Γ_0 is of class C^2 , the orthogonal projection P onto Γ_0 and thus $\mathbf{V}(\mathbf{x}, \omega)$ is at least of class
 418 C^1 , cf. [34]. Choosing c sufficiently small, we can guarantee that $\mathbf{V}(\Sigma, \omega) = \Sigma$. Finally, after

419 a possible scaling of the perturbation's amplitude, we can always guarantee that this choice
420 of \mathbf{V} satisfies the uniformity condition (9), cp. [43]. Now, assuming that

$$421 \quad \gamma_k := \left\| u_k \begin{bmatrix} \cos(\arg P \cdot) \\ \sin(\arg P \cdot) \end{bmatrix} B(\|\cdot - P \cdot\|_2) \right\|_{W^{1,\infty}(D_0, \mathbb{R}^2)}$$

422 is still in $\ell^1(\mathbb{N})$, we can carry over the regularity results from the previous section to our
423 forward model (19) one-to-one.

424 *Remark 12.* Since we aim at reconstructing the inclusion S from measurements of the
425 Neumann data at the fixed boundary Σ and since we impose that $\mathbf{V}(\Sigma, \omega) = \Sigma$, the Cauchy
426 data, i.e. Dirichlet data and Neumann data, are independent of the particular choice of the
427 blending function.

428 **4.1. Discretization.** Our approach to determine for the given pair $[\gamma_{0,\Sigma}^{\text{int}} q, \gamma_{0,\Gamma(\mathbf{y})}^{\text{int}} q] = [f, 0]$
429 the respective solution $q(\mathbf{x}, \mathbf{y})$ to (12) relies on the reformulation of the boundary value prob-
430 lem as a boundary integral equation by means of Green's fundamental solution

$$431 \quad k(\mathbf{x}, \mathbf{x}') = -\frac{1}{2\pi} \log \|\mathbf{x} - \mathbf{x}'\|_2.$$

432 Namely, the solution $q(\mathbf{x}, \mathbf{y})$ of (17) is given in each point $\mathbf{x} \in D(\mathbf{y})$ by Green's representation
433 formula

$$434 \quad (21) \quad q(\mathbf{x}, \mathbf{y}) = \int_{\Gamma(\mathbf{y}) \cup \Sigma} k(\mathbf{x}, \mathbf{x}') \gamma_1^{\text{int}} q(\mathbf{x}', \mathbf{y}) - \frac{\partial k(\mathbf{x}, \mathbf{x}')}{\partial \mathbf{n}_{\mathbf{x}'}} \gamma_0^{\text{int}} q(\mathbf{x}', \mathbf{y}) \, ds_{\mathbf{x}'}$$

435 Using the jump properties of the layer potentials, we arrive at the direct boundary integral
436 formulation which reads

$$437 \quad (22) \quad \frac{1}{2} \gamma_0^{\text{int}} q(\mathbf{x}, \mathbf{y}) = \int_{\Gamma(\mathbf{y}) \cup \Sigma} k(\mathbf{x}, \mathbf{x}') \gamma_1^{\text{int}} q(\mathbf{x}', \mathbf{y}) \, ds_{\mathbf{x}'} - \int_{\Gamma(\mathbf{y}) \cup \Sigma} \frac{\partial k(\mathbf{x}, \mathbf{x}')}{\partial \mathbf{n}_{\mathbf{x}'}} \gamma_0^{\text{int}} q(\mathbf{x}', \mathbf{y}) \, ds_{\mathbf{x}'},$$

438 where $\mathbf{x} \in \Gamma(\mathbf{y}) \cup \Sigma$. If we label the boundaries by $A, B \in \{\Gamma(\mathbf{y}), \Sigma\}$, then (22) includes the
439 single layer operator

$$440 \quad (23) \quad \mathcal{V} : C(A) \rightarrow C(B), \quad (\mathcal{V}_{AB} \rho)(\mathbf{x}) = -\frac{1}{2\pi} \int_A \log \|\mathbf{x} - \mathbf{x}'\|_2 \rho(\mathbf{x}') \, ds_{\mathbf{x}'},$$

441 and the double layer operator

$$442 \quad (24) \quad \mathcal{K} : C(A) \rightarrow C(B), \quad (\mathcal{K}_{AB} \rho)(\mathbf{x}) = \frac{1}{2\pi} \int_A \frac{\langle \mathbf{x} - \mathbf{x}', \mathbf{n}_{\mathbf{x}'} \rangle}{\|\mathbf{x} - \mathbf{x}'\|_2^2} \rho(\mathbf{x}') \, ds_{\mathbf{x}'},$$

443 with the densities $\rho \in C(A)$ being the Cauchy data of q on A . The equation (22) in combi-
444 nation with (23) and (24) indicates the Dirichlet-to-Neumann map, which for problem (12)
445 induces the following system of integral equations

$$446 \quad (25) \quad \begin{bmatrix} \mathcal{V}_{\Sigma\Sigma} & \mathcal{V}_{\Sigma\Gamma(\mathbf{y})} \\ \mathcal{V}_{\Gamma(\mathbf{y})\Sigma} & \mathcal{V}_{\Gamma(\mathbf{y})\Gamma(\mathbf{y})} \end{bmatrix} \begin{bmatrix} \rho_\Sigma \\ \rho_{\Gamma(\mathbf{y})} \end{bmatrix} = \begin{bmatrix} 1/2 \text{Id} + \mathcal{K}_{\Sigma\Sigma} & \mathcal{K}_{\Sigma\Gamma(\mathbf{y})} \\ \mathcal{K}_{\Gamma(\mathbf{y})\Sigma} & 1/2 \text{Id} + \mathcal{K}_{\Gamma(\mathbf{y})\Gamma(\mathbf{y})} \end{bmatrix} \begin{bmatrix} f \\ 0 \end{bmatrix}.$$

447 The boundary integral operator on the left hand side of this coupled system of boundary inte-
 448 gral equations is uniformly elliptic and continuous provided that $\text{diam}(D(\mathbf{y})) = \text{diam}(\Sigma) < 1$.
 449 This guarantees the unique solvability by the Lax-Milgram lemma.

450 For the approximation of the unknown Cauchy data, we use the collocation method based
 451 on trigonometric polynomials. Applying the trapezoidal rule for the numerical quadrature
 452 and the regularization technique along the lines of [35] to deal with the singular integrals,
 453 we arrive at an exponentially convergent Nyström method provided that the data and the
 454 boundaries and thus the solution are analytic. More precisely, we have the following result.

455 **Proposition 13.** *Let $\rho \in C^k(\partial D(\mathbf{y}))$ be the solution to (25). Then, there holds*

$$456 \quad \|\rho - \rho_n\|_{L^\infty(D(\mathbf{y}))} \leq Cn^{-k} \|\rho\|_{C^k(D(\mathbf{y}))},$$

457 where ρ_n is obtained from the Nyström method with $n = 2j$ points for some $j \in \mathbb{N}$.

458 *Proof.* For a proof of this statement, see [35]. ■

459 Thus, if the density ρ is even analytic, we arrive at the error estimate

$$460 \quad \|\rho - \rho_n\|_{L^\infty(D(\mathbf{y}))} \leq C \exp(-cn),$$

461 for some constants $C, c > 0$.

462 **5. Higher-Order Quasi-Monte Carlo.** In light of the recent development of higher-order
 463 quasi-Monte Carlo (QMC) methods, in particular so-called *interlaced polynomial lattice (IPL)*
 464 *rules* [12, 15, 23], and their application to problems in uncertainty quantification [13, 16, 21],
 465 we consider here the approximation of prior and posterior expectations by such deterministic
 466 QMC rules. IPL rules are adapted to the integrand function in a preprocessing step using the
 467 Component-by-Component (CBC) algorithm [38, 39], which requires as an input some bounds
 468 on the parametric derivatives of the integrand. By the analysis of the previous section, we
 469 have such bounds at our disposal.

470 We consider approximations of Z, Z' given in Theorem 1 and (6), respectively, where we
 471 assume a uniform prior distribution $\mu_0(d\mathbf{y}) = \prod_{k=1}^s dy_k$ on the truncated parameter sequence,
 472 which we denote here by $\mathbf{y}_{1:s}$. Given a collection $\mathcal{P}_N = \{\mathbf{y}_0, \dots, \mathbf{y}_{N-1}\} \subset [0, 1]^s$ of QMC points
 473 in s dimensions, the QMC approximation $\mathcal{Q}_{N,s}$ of the prior mean of a function $g: U \rightarrow \mathbb{R}$ is
 474 given by

$$475 \quad (26) \quad \mathbb{E}[g] = \int_U g(\mathbf{y}) \mu(d\mathbf{y}) \approx \mathcal{Q}_{N,s}[g] := \frac{1}{N} \sum_{n=0}^{N-1} g\left(\mathbf{y}_n - \frac{\mathbf{1}}{2}\right).$$

476 With the choices $g(\mathbf{y}) = \exp(-\Phi(\mathbf{y}, \delta))$ and $g(\mathbf{y}) = \phi(q(\mathbf{y})) \exp(-\Phi(\mathbf{y}, \delta))$, we obtain the
 477 integrals Z and Z' , which we approximate with (26). The posterior mean is then simply given
 478 as the ratio $\mathbb{E}^{\mu^\delta}[\phi \circ q] = Z'/Z$, see Theorem 1.

479 **5.1. Interlaced Polynomial Lattice Rules.** To give the points $\mathbf{y}_n, n = 0, \dots, N-1$,
 480 we require some definitions and notation. A polynomial lattice rule (without interlacing) is
 481 a rule with $N = b^m$ points for some prime b and a positive integer m , and is given by a
 482 *generating vector* \mathbf{q} whose components $q_j(x)$ are polynomials over the finite field \mathbb{Z}_b of degree

483 less than m . Let $\mathbb{Z}_b[x]$ denote the set of polynomials over \mathbb{Z}_b . We associate with each integer
 484 $n = 0, \dots, b^m - 1$ a polynomial $n(x) = \sum_{k=0}^{m-1} \xi_k x^k$, where ξ_k are the digits of n in base b , that
 485 is $n = \xi_0 + \xi_1 b + \xi_2 b^2 + \dots + \xi_{m-1} b^{m-1}$. To obtain points in $[0, 1]$ from the generating vector
 486 \mathbf{q} , we require the mapping $v_m: \mathbb{Z}_b(x^{-1}) \rightarrow [0, 1]$ given for integer w by

$$487 \quad v_m \left(\sum_{k=w}^{\infty} \xi_k x^{-k} \right) = \sum_{k=\max(1,w)}^m \xi_k b^{-k}.$$

488 For an irreducible polynomial $P \in \mathbb{Z}_b[x]$ of degree m , the j -th component of the n -th point of
 489 the point set \mathcal{P}_N is given by

$$490 \quad (\mathbf{y}_n)_j = v_m \left(\frac{n(x)q_j(x)}{P(x)} \right).$$

491 To obtain orders of convergence higher than one, we consider an additional interlacing step.
 492 To this end, we denote the digit interlacing function of $\alpha \in \mathbb{N}$ points as $D_\alpha: [0, 1)^\alpha \rightarrow [0, 1)$,

$$493 \quad D_\alpha(x_1, \dots, x_\alpha) = \sum_{a=1}^{\infty} \sum_{j=1}^{\alpha} \xi_{j,a} b^{-j-(a-1)\alpha},$$

494 where $\xi_{j,a}$ is the a -th digit in the expansion of the j -th point $x_j \in [0, 1)$ in base b^{-1} , $x_j =$
 495 $\xi_{j,1} b^{-1} + \xi_{j,2} b^{-2} + \dots$. For vectors in αs dimensions, digit interlacing is defined block-wise and
 496 denoted by $\mathcal{D}_\alpha: [0, 1)^{\alpha s} \rightarrow [0, 1)^s$ with

$$497 \quad \mathcal{D}_\alpha(x_1, \dots, x_{\alpha s}) = (D_\alpha(x_1, \dots, x_\alpha), D_\alpha(x_{\alpha+1}, \dots, x_{2\alpha}), \dots, D_\alpha(x_{(s-1)\alpha+1}, \dots, x_{s\alpha})).$$

498 For a generating vector $\mathbf{q} \in (\mathbb{Z}_b[x])^{\alpha s}$ containing α components for each of the s dimensions,
 499 the interlaced polynomial lattice point set is $\mathcal{D}_\alpha(\tilde{\mathcal{P}}_N) \subset [0, 1)^s$, where $\tilde{\mathcal{P}}_N \subset [0, 1)^{\alpha s}$ denotes
 500 the (classical) polynomial lattice point set in αs dimensions with generating vector \mathbf{q} . For
 501 more details on this method, see e.g. [12, 15, 23]. The following theorem states the higher order
 502 rates that are obtainable under suitable sparsity assumptions of the form stated in Section 2.

503 **Proposition 14 (Thm. 3.1 from [15]).** *For $m \geq 1$ and a prime b , let $N = b^m$ denote the*
 504 *number of QMC points. Let $s \geq 1$ and $\boldsymbol{\beta} = (\beta_j)_{j \geq 1}$ be a sequence of positive numbers, and let*
 505 *$\boldsymbol{\beta}_s = (\beta_j)_{1 \leq j \leq s}$ denote the first s terms. Assume that $\boldsymbol{\beta} \in \ell^p(\mathbb{N})$ for some $p < 1$.*

506 *If there exists a $c > 0$ such that a function F satisfies for $\alpha := \lfloor 1/p \rfloor + 1$ that*

$$507 \quad (27) \quad |(\partial_{\mathbf{y}}^\nu F)(\mathbf{y})| \leq c |\boldsymbol{\nu}|! \boldsymbol{\beta}_s^\nu \quad \text{for all } \boldsymbol{\nu} \in \{0, 1, \dots, \alpha\}^s, s \in \mathbb{N},$$

508 *then an interlaced polynomial lattice rule of order α with N points can be constructed in*
 509 *$\mathcal{O}(\alpha s N \log N + \alpha^2 s^2 N)$ operations, such that for the quadrature error holds*

$$510 \quad (28) \quad |I_s(F) - \mathcal{Q}_{N,s}(F)| \leq C_{\alpha, \boldsymbol{\beta}, b, p} N^{-1/p},$$

511 *where the constant $C_{\alpha, \boldsymbol{\beta}, b, p} < \infty$ is independent of s and N .*

512 **5.2. Combined Error Estimate.** As mentioned in Section 2, we consider three approxi-
 513 mations to the exact solution: dimension truncation, discretization of the partial differential
 514 equation (PDE), and quadrature approximation of the high-dimensional Bayesian integrals.

515 Combining Theorem 11 with (16) and considering the estimate (28) and Theorem 13, we
 516 obtain by the triangle inequality the following total error bound, where $p < 1$ denotes the
 517 summability of the sequence γ in a bound of the form (2) on the integrand function,

$$518 \quad |I[\phi(q)] - \mathcal{Q}_N[\phi(q_n^{(s)})]| \leq C(s^{-\theta(1/p-1)} + n^{-k} + N^{-1/p}),$$

519 where $C > 0$ is independent of the parametric dimension s , the number of discretization points
 520 n and the number of QMC points N .

521 6. Numerical Experiments.

522 **6.1. Setup.** We consider the parametric problem (12) with the uncertain domain bound-
 523 ary $\Gamma(\omega)$ parametrized as described in Section 4. More precisely, we shall impose that the
 524 Karhunen-Loève expansion is given by a Fourier series with random coefficients, i.e.

$$525 \quad u(\varphi, \omega) = u_0(\varphi) + \sigma \sum_{k=1}^{\infty} Y_k(\omega) u_k(\varphi).$$

526 Letting $Y_k \in [-1/2, 1/2]$ be uniformly distributed, we can identify the random variables
 527 $\{Y_k\}_k$ by their image $\mathbf{y} \in U = [-1/2, 1/2]^{\mathbb{N}}$. We additionally assume a constant nominal
 528 value $u_0(\varphi) \equiv u_0 \in (0, \infty)$ and write $u_{2k}(\varphi) = \vartheta_{2k} \cos(k\varphi)$ and $u_{2k-1} = \vartheta_{2k-1} \sin(k\varphi)$ yielding
 529 the parametric representation

$$530 \quad (29) \quad u(\varphi, \mathbf{y}) = u_0 + \sigma \sum_{k=1}^{\infty} y_k u_k(\varphi),$$

531 where we choose throughout the following $u_0 = 0.3$, $\sigma = 0.125$ and $\vartheta_{2k} = \vartheta_{2k-1} = k^{-\zeta}$. The
 532 last choice enforces the decay $\sup_{\varphi} |u_k(\varphi)| \leq Ck^{-\zeta}$ where we choose $\zeta = 4$, implying that
 533 the unknown boundary Γ of the inclusion is at least four times continuously differentiable.
 534 We truncate the sum (29) at $s = 100$ terms, and are interested in the convergence of the
 535 QMC approximation to the resulting 100-dimensional integral with respect to the number of
 536 quadrature points.

537 In the present context, considering the parametrization (18), we will be interested in
 538 computing prior ($\mu = \mu_0$) and posterior ($\mu = \mu^\delta$) expectation and variance,

$$539 \quad (30) \quad \mathbb{E}^\mu[\Gamma(\mathbf{y})] = \{\mathbf{x} \in \mathbb{R}^2 : \mathbf{x} = \mathbb{E}^\mu[u(t, \mathbf{y})]\mathbf{e}(t), t \in I\}$$

$$540 \quad (31) \quad \mathbb{V}^\mu[\Gamma(\mathbf{y})] = \{\mathbf{x} \in \mathbb{R}^2 : \mathbf{x} = \mathbb{V}^\mu[u(t, \mathbf{y})]\mathbf{e}(t), t \in I\}.$$

542 Based on the analysis in Section 2.2, we consider higher-order quasi-Monte Carlo with
 543 smoothness-driven product and order dependent (SPOD) weights, as introduced in [15]. For
 544 the experiments presented here, we used generating vectors constructed by the fast CBC
 545 method and made available in [22], with parameters $\alpha = \zeta$, sequence $\beta_j = \sigma\vartheta_j$, and Walsh
 546 coefficient bound $C = 0.1$. The construction was executed for $\zeta \in \{2, 3, 4\}$; see below for

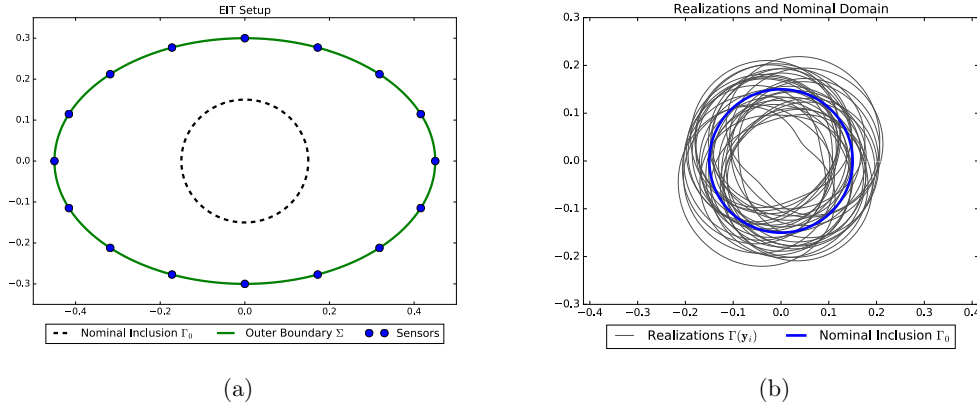


Figure 2: **a** Simulation setup with outer boundary Σ , the nominal inner boundary Γ_0 , and locations of the $K = 16$ sensors. **b** Realizations of the inclusion $\Gamma(\mathbf{y})$ resulting from the IPL point set with $m = 5$.

547 a discussion of the different cases. See also [21] for more computational details on CBC
 548 construction of IPL rules and the mentioned parameters. For the implementation, we used a
 549 custom boundary integral solver coupled with the `gMLQMC` library [20] for applying higher-order
 550 QMC.

551 As observation operator \mathcal{O} , we consider the evaluation of the solution's Neumann data
 552 $\partial q / \partial \mathbf{n}$ in $K = 16$ equi-spaced points (with respect to the angle) on the outer boundary Σ , and
 553 thus $\delta = \mathcal{O}(q) + \eta \in \mathbb{R}^{16}$. As quantity of interest, we are interested in the interior boundary,
 554 which we represent as a vector of radius values of length M , for equispaced points in the angle
 555 φ . Thus, the QoI $\phi(q(\mathbf{y})) \in \mathbb{R}^M$ is, for each parameter vector \mathbf{y} , a discrete approximation of
 556 the shape of the inclusion. Figure 2 shows a setup of the experiment with the enclosing ellipse
 557 Σ (semiaxes 0.45 and 0.3), the nominal domain Γ_0 , and various realizations of the parametric
 558 domain $\Gamma(\mathbf{y})$. Finally, the prescribed Dirichlet data at Σ are given by $g_D(\mathbf{x}) = x_1^2 - x_2^2$.

559 **6.2. Results.** The prior and posterior expectations of the domain shape are given in
 560 Figure 3, which shows that incorporation of measurement data gives a reasonable estimate
 561 of the “true” shape. Moreover, the Bayesian framework allows specification of a confidence
 562 interval to assess the inherent uncertainty in the model and measurement process; in this
 563 example, the true shape is fully contained in the 1σ -confidence interval around the posterior
 564 mean, whereas the prior mean deviates significantly.

565 We are particularly interested in the verification of convergence rates of the approximations
 566 to the high-dimensional integrals Z and Z' from Theorem 1 and (6) using interlaced polynomial
 567 lattice rules (IPL). The prior expectation of the inclusion's shape in this case does not depend
 568 on the solution to the PDE (17); moreover, it is by the parametrization (20) simply an affine
 569 function of the parameters y_j . Prescribing a decay $\zeta = 4$, we thus expect due to (28) a

570 convergence rate of N^{-4} for the prior expectation, for interlacing factor $\alpha = 4$. In the case
 571 where the QoI depends on the solution, the condition that the sequence of $W^{1,\infty}$ -norms in γ_k
 572 from (10) is summable implies the loss of one order of convergence, which would imply the
 573 rate N^{-3} for the prior approximation, and the use of $\zeta = 3$ also in the CBC construction.
 574 For the posterior, Theorem 4 implies an additional loss of one order of convergence; assuming
 575 the condition in (2) on the parameter-to-solution map $G: \mathbf{y} \rightarrow q(\mathbf{y}; \cdot)$ for $1/\zeta < p < 1/3$, we
 576 thus obtain an expected higher-order QMC convergence rate of $N^{-\zeta+2}$. For the case of $\zeta = 4$
 577 considered here, we thus expect N^{-2} when using IPL rules with interlacing factor $\alpha \geq 2$. We
 578 note that the generating vectors used in the posterior mean approximation were based on
 579 $\zeta = 2$ with interlacing factor $\alpha = 2$.

580 We consider both the prior and posterior expectations of the quantity of interest ϕ , which,
 581 as described above, yields a discrete approximation of the boundary $r_{\mathbf{y}}(\varphi)$ with M points
 582 $\varphi_1, \dots, \varphi_M$. We compute the error by approximating the L^2 -norm over the angle φ , given for
 583 the prior by

$$584 \quad (32) \quad \begin{aligned} \|\mathbb{E}^{\mu_0} - \mathcal{Q}_N[r_{\mathbf{y}}(\cdot)]\|_{L^2([0,2\pi])}^2 &= \int_0^{2\pi} \left(\mathbb{E}^{\mu_0}[r_{\mathbf{y}}(\varphi)] - \mathcal{Q}_N[r_{\mathbf{y}}(\varphi)] \right)^2 d\varphi \\ 585 &\approx \frac{1}{M} \sum_{i=1}^M \left(\mathbb{E}^{\mu_0}[r_{\mathbf{y}}(\varphi_i)] - \mathcal{Q}_N[r_{\mathbf{y}}(\varphi_i)] \right)^2, \\ 586 \end{aligned}$$

587 and analogously for the posterior mean \mathbb{E}^{μ^δ} over $\mathbf{y} \in U$. Due to the lack of an analytically
 588 given exact solution, we use a reference solution computed with $N = 2^{20}$ points using an
 589 interlaced polynomial lattice (IPL) rule, and consider in the following convergence plots the
 590 values $N = 2^k$ for $k = 1, \dots, 19$. As a comparison to IPL rules, we also compute Halton and
 591 “plain vanilla” Monte Carlo (MC) estimates of the involved integrals for the same values of
 592 N , where the expected convergence rates in this case are N^{-1} and $N^{-1/2}$, respectively. For
 593 MC, we approximate the L^2 -error by averaging over $R = 10$ repetitions.

594 Figures 4 and 5 show the convergence of approximations to the prior and posterior ex-
 595 pectation obtained using the methods mentioned above. A linear least squares fit is included
 596 to measure the convergence rate; the points used in the fit correspond to the points at which
 597 the linear fit is evaluated. Note that in Figure 4, the prior expectation does not involve the
 598 solution of the PDE, thus we obtain the full rate $N^{-\zeta}$. If the QoI were to depend on the
 599 solution $q(\mathbf{y})$, we would expect a rate $N^{-\zeta+1}$. In Figure 5, various values of the observation
 600 noise covariance Γ are considered. For small Γ , concentration effects cause the performance
 601 of the methods to deteriorate, as is to be expected, see e.g. [41]. The expected IPL rate here
 602 is N^{-2} , which can be seen for large Γ .

603 **7. Conclusion.** In this article we have described the application of higher-order Quasi-
 604 Monte Carlo methods to a Bayesian approach for shape uncertainty quantification based on
 605 a parametric partial differential equation forward model. In particular, we have established a
 606 rigorous analysis of the posterior measure and a truncation analysis for the forward model. The
 607 presented bounds on mixed partial derivatives of the posterior imply higher-order convergence
 608 rates of the quadrature error versus the number of nodes. The obtained convergence rates
 609 depend on the quantity of interest and choice of either prior or posterior measure. Numerical

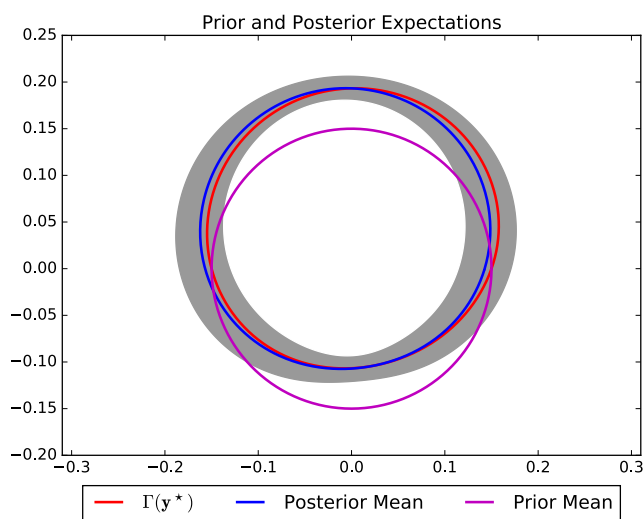


Figure 3: Prior and posterior expectations of the inclusion for $\Gamma = (0.1)^2$. The grey shaded area is a 1σ -confidence interval, which in this case contains the “truth” $\Gamma(\mathbf{y}^*)$. It can be seen that the prior expectation deviates significantly from $\Gamma(\mathbf{y}^*)$.

610 results conducted for an elliptic equation arising in Electrical Impedance Tomography confirm
 611 the theoretically derived rates in $s = 100$ parametric dimensions. A comparison with Halton
 612 and Monte Carlo sampling shows the superiority of the applied interlaced polynomial lattice
 613 rules in the case where the observation noise covariance is not too small.

614 *Acknowledgments.* We would like to thank Christoph Schwab for suggesting the present
 615 analysis and Helmut Harbrecht for the fruitful discussions and many helpful remarks.

616 **Appendix A. Multivariate Combinatorics.** We start this section by defining the arith-
 617 metic for multi-indices. To that end, let $\alpha, \beta \in \mathbb{N}^s$ for some $s \in \mathbb{N}$ with $s \geq 1$. The set
 618 of natural numbers is always supposed to include the element 0, i.e. $0 \in \mathbb{N}$. We define the
 619 addition and subtraction of two multi-indices in the canonical way. Moreover, we define

$$620 \quad \alpha^\beta := \alpha_1^{\beta_1} \cdots \alpha_s^{\beta_s}$$

621 with the convention $0^0 = 1$. The modulus of α is given by

$$622 \quad |\alpha| := \sum_{i=1}^s \alpha_i$$

623 and its factorial is defined according to

$$624 \quad \alpha! := \alpha_1! \cdots \alpha_s!.$$

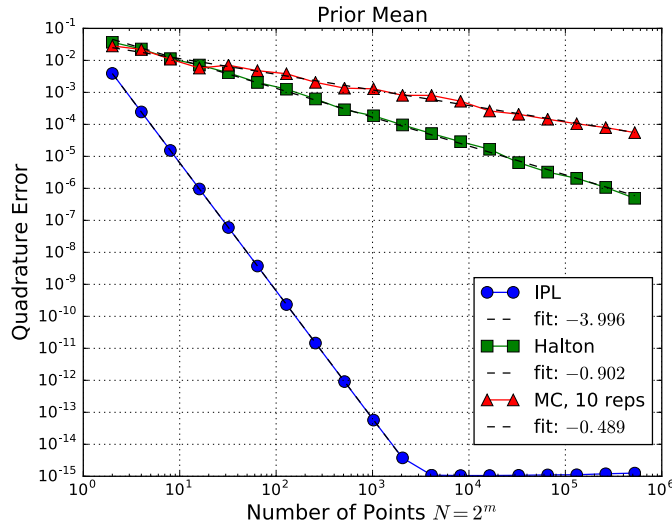


Figure 4: Approximations to the prior expectation with IPL, Halton and MC rules. The expected rates are N^{-4} for IPL, N^{-1} for Halton and $N^{-1/2}$ for MC, which are all confirmed by these results.

625 Then, we can also define the multivariate binomial coefficient

$$626 \quad \binom{\alpha}{\beta} := \frac{\alpha!}{(\alpha - \beta)! \beta!},$$

627 where we assume $\beta \leq \alpha$ and the relation \leq has to be understood component-wise.

628 The following lemma is a special case of formula (7.4) in [9].

629 **Lemma 15.** Let $\gamma = \{\gamma_k\}_k \in \ell^1(\mathbb{N})$ with $\gamma_k \geq 0$. Moreover, assume that $c_\gamma := \|\gamma\|_{\ell^1} < 1$.
630 Then, it holds

$$631 \quad \sum_{\nu} \frac{|\nu|!}{\nu!} \gamma^\nu = \frac{1}{1 - c_\gamma} \quad \text{for all } \nu \in \mathcal{F}.$$

632 and therefore there exists a constant with $|\nu|!/\nu! \gamma^\nu \leq c$ for all $\nu \in \mathcal{F}$.

633 *Proof.* Let $\mathcal{F}^{(s)} := \{\nu \in \mathcal{F} : \nu_k = 0 \text{ for all } k > s\}$. Then, we have obviously $\mathcal{F} = \cup_{s \in \mathbb{N}} \mathcal{F}^{(s)}$.

634 Now, there holds for all $\nu \in \mathcal{F}^{(s)}$ that

$$635 \quad \sum_{\nu} \frac{|\nu|!}{\nu!} \gamma^\nu = \sum_{k=0}^{\infty} \sum_{|\nu|=k} \frac{k!}{\nu!} \gamma^\nu = \sum_{k=0}^{\infty} \left(\sum_{j=1}^s \gamma_j \right)^k \leq \sum_{k=0}^{\infty} c_\gamma^k = \frac{1}{1 - c_\gamma}$$

636 by the multinomial theorem and the limit of the geometric series. Since the derived bound is
637 uniform in the support size $s \in \mathbb{N}$ of the index sequences, we arrive at the assertion. ■

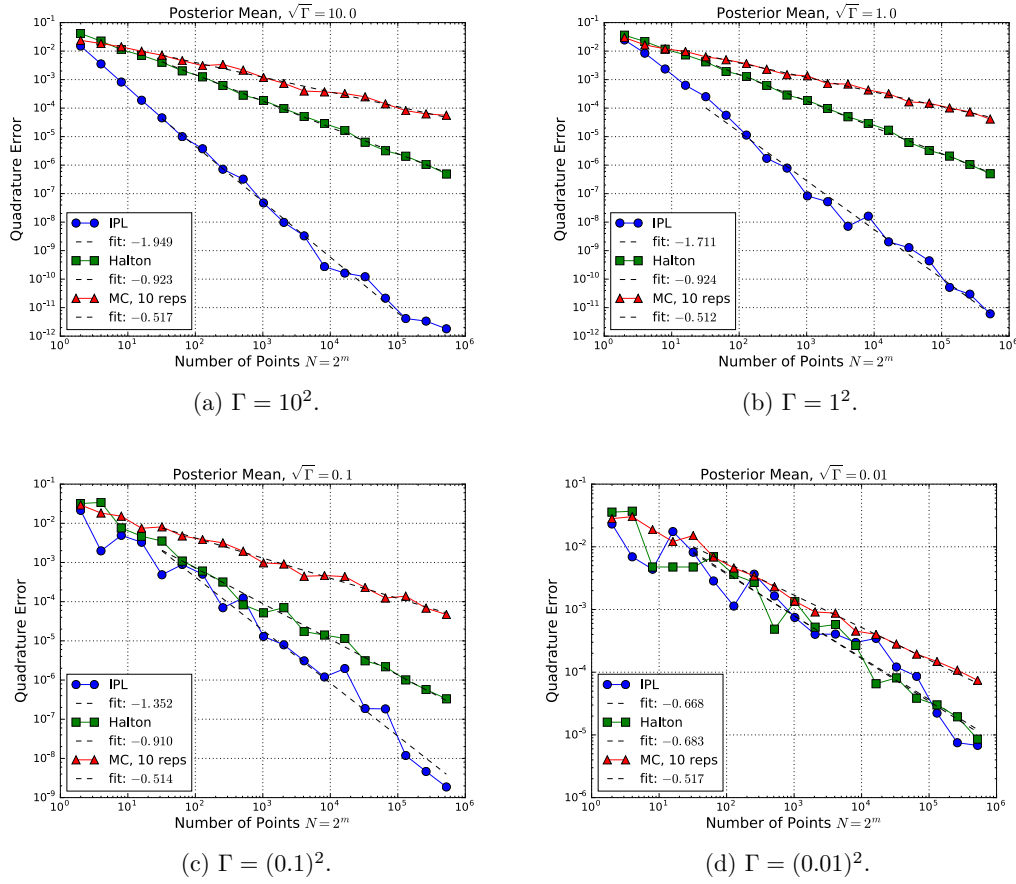


Figure 5: Convergence of IPL, Halton and MC approximations to the posterior expectation for different Γ , with the error computed as in (32) wrt. a reference solution with $N = 2^{20}$ IPL points.

638 **Lemma 16.** For all $\alpha, \beta, r \in \mathbb{N}$ with $r > 0$ it holds

639
$$\binom{\alpha + r - 1}{r - 1} \binom{\beta + r - 1}{r - 1} \leq \frac{(\alpha + \beta)!}{\alpha! \beta!} \binom{\alpha + \beta + r - 1}{r - 1}.$$

640 *Proof.* It holds

$$\begin{aligned}
641 & \binom{\alpha+r-1}{r-1} \binom{\beta+r-1}{r-1} \leq \frac{(\alpha+\beta)!}{\alpha!\beta!} \binom{\alpha+\beta+r-1}{r-1} \\
642 & \iff \binom{\alpha+r-1}{r-1} \frac{(\beta+r-1)!}{\beta!(r-1)!} \leq \frac{(\alpha+\beta)!}{\alpha!\beta!} \frac{(\alpha+\beta+r-1)!}{(\alpha+\beta)!(r-1)!} \\
643 & \iff \binom{\alpha+r-1}{r-1} (\beta+r-1)! \leq \frac{(\alpha+\beta+r-1)!}{\alpha!} \\
644 & \iff \binom{\alpha+r-1}{r-1} \leq \binom{\alpha+\beta+r-1}{\beta+r-1}.
\end{aligned}$$

646 The last inequality is true due to the monotonically increasing diagonals in Pascal's triangle.
647 This proves the assertion. ■

648 **Lemma 17.** *It holds for $\alpha \in \mathbb{N}^s$, $\alpha' \in \mathbb{N}^{s'}$ that*

$$649 \quad \prod_{i=1}^s \binom{\alpha_i + |\alpha'| - 1}{|\alpha'| - 1} \leq \frac{|\alpha'|!}{\alpha!} \binom{|\alpha| + |\alpha'| - 1}{|\alpha'| - 1}.$$

650 *Proof.* The proof is by induction on s . For $s = 1$, we have

$$651 \quad \binom{\alpha_1 + |\alpha'| - 1}{|\alpha'| - 1} = \frac{\alpha_1!}{\alpha_1!} \binom{\alpha_1 + |\alpha'| - 1}{|\alpha'| - 1},$$

652 which holds with equality. Let the induction hypothesis be valid for $s - 1$ and set $\alpha_{s-1} =$
653 $[\alpha_1, \dots, \alpha_{s-1}]$. Then, we derive with the previous lemma that

$$\begin{aligned}
& \prod_{i=1}^s \binom{\alpha_i + |\alpha'| - 1}{|\alpha'| - 1} \leq \frac{|\alpha_{s-1}|!}{\alpha_{s-1}!} \binom{|\alpha_{s-1}| + |\alpha'| - 1}{|\alpha'| - 1} \binom{\alpha_s + |\alpha'| - 1}{r-1} \\
& \leq \frac{|\alpha_{s-1}|!}{\alpha_{s-1}!} \frac{(|\alpha_{s-1}| + \alpha_s)!}{|\alpha_{s-1}|\alpha_s!} \binom{|\alpha_{s-1}| + \alpha_s + |\alpha'| - 1}{|\alpha'| - 1} \\
654 & = \frac{|\alpha'|!}{\alpha!} \binom{|\alpha| + |\alpha'| - 1}{|\alpha'| - 1}. \quad \blacksquare
\end{aligned}$$

655 REFERENCES

- 656 [1] M. ABRAMOWITZ AND I. A. STEGUN, *Handbook of Mathematical Functions: With Formulas, Graphs, and*
657 *Mathematical Tables*, Applied mathematics series, Dover Publications, N. Chemsford, MA, 1964.
658 [2] I. AKDUMAN AND R. KRESS, *Electrostatic imaging via conformal mapping*, *Inverse Problems*, 18 (2002),
659 p. 1659.
660 [3] G. ALESSANDRINI, V. ISAKOV, AND J. POWELL, *Local uniqueness in the inverse conductivity problem with*
661 *one measurement*, *Transactions of the American Mathematical Society*, 347 (1995), pp. 3031–3041.
662 [4] J. BECK, R. TEMPONE, F. NOBILE, AND L. TAMELLINI, *On the optimal polynomial approximation of*
663 *stochastic PDEs by Galerkin and collocation methods*, *Mathematical Models and Methods in Applied*
664 *Sciences*, 22 (2012), pp. 1250023.

- 665 [5] M. BRÜHL, *Explicit characterization of inclusions in Electrical Impedance Tomography*, SIAM Journal on
666 Mathematical Analysis, 32 (2001), pp. 1327–1341.
- 667 [6] J. E. CASTRILLON-CANDAS, F. NOBILE, AND R. F. TEMPONE, *Analytic regularity and collocation ap-*
668 *proximation for elliptic PDEs with random domain deformations*, Computers & Mathematics with
669 Applications, 71 (2016), pp. 1173 – 1197.
- 670 [7] R. CHAPKO AND R. KRESS, *A hybrid method for inverse boundary value problems in potential theory*,
671 Journal of Inverse and Ill-posed Problems, 13 (2005), pp. 27–40.
- 672 [8] P. CHEN AND C. SCHWAB, *Adaptive sparse grid model order reduction for fast Bayesian estimation and*
673 *inversion*, in Sparse Grids and Applications - Stuttgart 2014, J. Garcke and D. Pflüger, eds., Cham,
674 2016, Springer International Publishing, pp. 1–27, doi:10.1007/978-3-319-28262-6_1, [http://dx.doi.](http://dx.doi.org/10.1007/978-3-319-28262-6_1)
675 [org/10.1007/978-3-319-28262-6_1](http://dx.doi.org/10.1007/978-3-319-28262-6_1).
- 676 [9] A. COHEN, R. DEVORE, AND C. SCHWAB, *Convergence rates of best N -term Galerkin approximations*
677 *for a class of elliptic sPDEs*, Foundations of Computational Mathematics, 10 (2010).
- 678 [10] G. M. CONSTANTINE AND T. H. SAVITS, *A multivariate Faà di Bruno formula with applications*, Trans-
679 actions of the American Mathematical Society, 248 (1996), pp. 503–520.
- 680 [11] M. DASHTI AND A. M. STUART, *The Bayesian approach to inverse problems*, (to appear in Springer
681 Handbook of Uncertainty Quantification), (2013), arXiv:arXiv:1302.6989.
- 682 [12] J. DICK, *Walsh spaces containing smooth functions and quasi-Monte Carlo rules of arbitrary high order*,
683 SIAM Journal on Numerical Analysis, 46 (2008), pp. 1519–1553, doi:10.1137/060666639, [http://dx.](http://dx.doi.org/10.1137/060666639)
684 [doi.org/10.1137/060666639](http://dx.doi.org/10.1137/060666639).
- 685 [13] J. DICK, R. N. GANTNER, Q. T. LE GIA, AND C. SCHWAB, *Higher order quasi-Monte Carlo inte-*
686 *gration for Bayesian estimation*, Tech. Report 2016-13, Seminar for Applied Mathematics, ETH
687 Zürich, Switzerland, 2016, [https://www.sam.math.ethz.ch/sam_reports/reports/reports_final/reports2016/](https://www.sam.math.ethz.ch/sam_reports/reports_final/reports2016/2016-13.pdf)
688 [2016-13.pdf](https://www.sam.math.ethz.ch/sam_reports/reports/reports_final/reports2016/2016-13.pdf).
- 689 [14] J. DICK, R. N. GANTNER, Q. T. LE GIA, AND C. SCHWAB, *Multilevel higher order quasi-Monte Carlo*
690 *Bayesian estimation*, Tech. Report 2016-34, Seminar for Applied Mathematics, ETH Zürich, Switzer-
691 land, 2016, https://www.sam.math.ethz.ch/sam_reports/reports_final/reports2016/2016-34.pdf.
- 692 [15] J. DICK, F. Y. KUO, Q. T. LE GIA, D. NUYENS, AND C. SCHWAB, *Higher order QMC Petrov-Galerkin*
693 *discretization for affine parametric operator equations with random field inputs*, SIAM Journal on
694 Numerical Analysis, 52 (2014), p. 2676–2702, doi:10.1137/130943984, [http://dx.doi.org/10.1137/](http://dx.doi.org/10.1137/130943984)
695 [130943984](http://dx.doi.org/10.1137/130943984).
- 696 [16] J. DICK, Q. T. LE GIA, AND C. SCHWAB, *Higher order quasi-Monte Carlo integration for holomorphic,*
697 *parametric operator equations*, SIAM/ASA Journal on Uncertainty Quantification, 4 (2016), p. 48–79,
698 doi:10.1137/140985913, <http://epubs.siam.org/doi/10.1137/140985913> (accessed 2016-07-05).
- 699 [17] M. M. DUNLOP AND A. M. STUART, *The Bayesian formulation of EIT: Analysis and algorithms*, arXiv
700 preprint arXiv:1508.04106, (2015).
- 701 [18] K. EPPLER AND H. HARBRECHT, *A regularized Newton method in Electrical Impedance Tomography using*
702 *shape Hessian information*, Control and Cybernetics, 34 (2005), pp. 203–225.
- 703 [19] A. FRIEDMAN AND V. ISAKOV, *On the uniqueness in the inverse conductivity problem with one measure-*
704 *ment*, Indiana University Mathematics Journal, 38 (1989), pp. 563–579.
- 705 [20] R. N. GANTNER, *A generic C++ library for multilevel quasi-Monte Carlo*, in Proceedings of the Platform
706 for Advanced Scientific Computing Conference, PASC '16, New York, NY, USA, 2016, ACM, pp. 11:1–
707 11:12, doi:10.1145/2929908.2929915.
- 708 [21] R. N. GANTNER AND C. SCHWAB, *Computational higher order quasi-Monte Carlo integration*, in Monte
709 Carlo and Quasi-Monte Carlo Methods: MCQMC, Leuven, Belgium, April 2014, R. Cools and
710 D. Nuyens, eds., Springer International Publishing, Cham, 2016, pp. 271–288, doi:10.1007/978-3-
711 [319-33507-0_12](https://doi.org/10.1007/978-3-319-33507-0_12).
- 712 [22] R. N. GANTNER AND C. SCHWAB, *Generating vector repository*. [http://www.sam.math.ethz.ch/](http://www.sam.math.ethz.ch/HOQMC/genvecs/)
713 [HOQMC/genvecs/](http://www.sam.math.ethz.ch/HOQMC/genvecs/), 2016. Accessed: 2016-08-05.
- 714 [23] T. GODA AND J. DICK, *Construction of interlaced scrambled polynomial lattice rules of arbitrary high*
715 *order*, Foundations of Computational Mathematics. The Journal of the Society for the Foundations
716 of Computational Mathematics, 15 (2015), pp. 1245–1278, doi:10.1007/s10208-014-9226-8, [http://dx.](http://dx.doi.org/10.1007/s10208-014-9226-8)
717 [doi.org/10.1007/s10208-014-9226-8](http://dx.doi.org/10.1007/s10208-014-9226-8).
- 718 [24] H. HARBRECHT AND T. HOHAGE, *A Newton method for reconstructing non star-shaped domains in Elec-*

- 719 *trical Impedance Tomography*, Inverse Problems and Imaging, 3 (2009), pp. 353–371.
- 720 [25] H. HARBRECHT AND M. PETERS, *Solution of free boundary problems in the presence of geometric uncer-*
 721 *tainties*, Preprint 2015-02, Mathematisches Institut, Universität Basel, (2015). to appear in Radon
 722 Series on Computational and Applied Mathematics, de Gruyter.
- 723 [26] H. HARBRECHT, M. PETERS, AND M. SIEBENMORGEN, *Efficient approximation of random fields for*
 724 *numerical applications*, Numerical Linear Algebra with Applications, 22 (2015), pp. 596–617.
- 725 [27] H. HARBRECHT, M. PETERS, AND M. SIEBENMORGEN, *Analysis of the domain mapping method for*
 726 *elliptic diffusion problems on random domains*, Numerische Mathematik, (2016), pp. 1–34.
- 727 [28] F. HETTLICH AND W. RUNDELL, *The determination of a discontinuity in a conductivity from a single*
 728 *boundary measurement*, Inverse Problems, 14 (1998), p. 67.
- 729 [29] S. HEUBACH AND T. MANSOUR., *Combinatorics of Compositions and Words*, CRC Press, Boca Raton,
 730 2009.
- 731 [30] N. HIGHAM, *Accuracy and Stability of Numerical Algorithms*, Society for Industrial and Applied Mathe-
 732 matics, Philadelphia, 2002.
- 733 [31] E. HILLE AND R. S. PHILLIPS, *Functional Analysis and Semi-Groups*, vol. 31, American Mathematical
 734 Society, Providence, 1957.
- 735 [32] V. H. HOANG, C. SCHWAB, AND A. M. STUART, *Complexity analysis of accelerated MCMC methods for*
 736 *Bayesian inversion*, Inverse Problems, 29 (2013), pp. 085010, 37, doi:10.1088/0266-5611/29/8/085010,
 737 <http://dx.doi.org/10.1088/0266-5611/29/8/085010>.
- 738 [33] D. S. HOLDER, *Electrical Impedance Tomography: Methods, History and Applications*, CRC Press, Boca
 739 Raton, 2004.
- 740 [34] R. B. HOLMES, *Smoothness of certain metric projections on Hilbert space*, Transactions of the American
 741 Mathematical Society, 184 (1973), pp. 87–100.
- 742 [35] R. KRESS, *Linear integral equations*, Vol. 82 of Applied Mathematical Sciences, Springer, New York,
 743 2nd ed., 1999.
- 744 [36] F. Y. KUO, C. SCHWAB, AND I. H. SLOAN, *Quasi-Monte Carlo Methods for High-Dimensional Integration:*
 745 *the Standard (Weighted Hilbert Space) Setting and Beyond*, The ANZIAM Journal, 53 (2012), p. 251,
 746 doi:10.1017/S1446181112000144, http://www.journals.cambridge.org/abstract_S1446181112000144.
- 747 [37] M. LOÈVE, *Probability Theory. I+II*, no. 45 in Graduate Texts in Mathematics, Springer, New York,
 748 4th ed., 1977.
- 749 [38] D. NUYENS AND R. COOLS, *Fast algorithms for component-by-component construction of rank-1 lattice*
 750 *rules in shift-invariant reproducing kernel Hilbert spaces*, Mathematics of Computation, 75 (2006),
 751 p. 903–920 (electronic), doi:10.1090/S0025-5718-06-01785-6.
- 752 [39] D. NUYENS AND R. COOLS, *Fast component-by-component construction, a reprise for different kernels*, in
 753 Monte Carlo and quasi-Monte Carlo methods 2004, Springer, Berlin, 2006, p. 373–387, doi:10.1007/3-
 754 540-31186-6_22, http://dx.doi.org/10.1007/3-540-31186-6_22.
- 755 [40] C. SCHILLINGS AND C. SCHWAB, *Sparsity in Bayesian inversion of parametric operator equations*, Inverse
 756 Problems, 30 (2014), pp. 065007, 30, doi:10.1088/0266-5611/30/6/065007, <http://dx.doi.org/10.1088/0266-5611/30/6/065007>.
- 757 [41] C. SCHILLINGS AND C. SCHWAB, *Scaling limits in computational Bayesian inversion*, ESAIM: Mathemat-
 758 ical Modelling and Numerical Analysis (to appear), (2016), doi:10.1051/m2an/2016005.
- 760 [42] C. SCHWAB AND R. TODOR, *Karhunen-Loève approximation of random fields by generalized fast multipole*
 761 *methods*, Journal of Computational Physics, 217 (2006), pp. 100–122.
- 762 [43] J. SIMON, *Differentiation with respect to the domain in boundary value problems*, Numerical Functional
 763 Analysis and Optimization, 2 (1980), pp. 649–687.
- 764 [44] D. XIU AND D. M. TARTAKOVSKY, *Numerical methods for differential equations in random domains*,
 765 SIAM Journal on Scientific Computing, 28 (2006), pp. 1167–1185.

LATEST PREPRINTS

No.	Author: Title
2015-36	J. K. Canci <i>Good reduction for endomorphisms of the projective line in terms of the branch locus</i>
2015-37	J. K. Canci, L. Paladino <i>Preperiodic points for rational functions defined over a global field in terms of good reduction</i>
2015-38	J. K. Canci <i>Preperiodic points for rational functions defined over a rational function field of characteristic zero</i>
2015-39	J. K. Canci, S. Vishkautsan <i>Quadratic maps with a periodic critical point of period 2</i>
2015-40	H. Harbrecht, M. Peters <i>The second order perturbation approach for PDEs on random domains</i>
2015-41	H. Harbrecht, W. L. Wendland, N. Zorii <i>Minimal energy problems for strongly singular Riesz kernels</i>
2015-42	H. Harbrecht, M. Utzinger <i>On adaptive wavelet boundary element methods</i>
2016-01	S. Iula, G. Mancini <i>Extremal functions for singular Moser-Trudinger embeddings</i>
2016-02	J. K. Canci, L. Paladino <i>On preperiodic points of rational functions defined over $\mathbb{F}_p(t)$</i>
2016-03	H. Harbrecht, R. Schneider <i>A note on multilevel based error estimation</i>
2016-04	C. Urech <i>On homomorphisms between Cremona groups</i>
2016-05	A. P. Choudhury, H. Heck <i>Stability of the inverse boundary value problem for the biharmonic operator: Logarithmic estimates</i>
2016-06	M. Dambrine, I. Greff, H. Harbrecht, B. Puig <i>Numerical solution of the homogeneous Neumann boundary value problem on domains with a thin layer of random thickness</i>

LATEST PREPRINTS

No.	Author:	Title
2016-07	G. Alberti, G. Crippa, A. L. Mazzucato	<i>Exponential self-similar mixing by incompressible flows</i>
2016-08	M. Bainbridge, P. Habegger, M. Möller	<i>Teichmüller curves in genus three and just likely intersections in $G_m^n \times G_a^n$</i>
2016-09	Gabriel A. Dill	<i>Effective approximation and Diophantine applications</i>
2016-10	J. Blanc, S. Zimmermann	<i>Topological simplicity of the Cremona groups</i>
2016-11	I. Hedén, S. Zimmermann	<i>The decomposition group of a line in the plane</i>
2016-12	J. Ballani, D. Kressner, M. Peters	<i>Multilevel tensor approximation of PDEs with random data</i>
2016-13	M. J. Grote, M. Kray, U. Nahum	<i>Adaptive eigenspace method for inverse scattering problems in the frequency domain</i>
2016-14	H. Harbrecht, M. Peters, M. Schmidlin	<i>Uncertainty quantification for PDEs with anisotropic random diffusion</i>
2016-15	F. Da Lio, L. Martinazzi	<i>The nonlocal Liouville-type equation in R and conformal immersions of the disk with boundary singularities</i>
2016-16	A. Hyder	<i>Conformally Euclidean metrics on R^n with arbitrary total Q-curvature</i>
2016-17	G. Mancini, L. Martinazzi	<i>The Moser-Trudinger inequality and its extremals on a disk via energy estimates</i>
2016-18	R. N. Gantner, M. D. Peters	<i>Higher order quasi-Monte Carlo for Bayesian shape inversion</i>